Scientific Research Publishing

Journal of Electromagnetic Analysis and Applications, 2026, 18(10), 175-216
https://www.scirp.org/journal/jemaa
ISSN Online: 1942-0749
ISSN Print: 1942-0730

Comparative Analysis and Modeling of 4G LTE Propagation Using the Okumura-Hata and COST-231 Hata Models, Enhanced with Spatially Correlated Log-Normal Shadowing

Kadiatou Aissatou Barry[1,2,3], Mohamed Ansoumane Camara[1,2], Boudal Niang[3], Mamadou Sadigou Diallo[1,2], Ismaila Diakhaté[3], Souleymane Soumah[1,2,4]

[1]Polytechnic Institute of Gamal Abdel Nasser University of Conakry (IP-UGANC), Conakry, Guinea
[2]Laboratory for Teaching and Research in Energy, Automation and Telecommunications (LENAT), UGANC, Conakry, Guinea
[3]Laboratory for Research in Digital Science and Technology (LRSTN), ESMT, Dakar, Senegal
[4]Water, Energy, Environment and Industrial Processes Laboratory (LE3PI), Cheikh Anta Diop University, Dakar, Senegal
Email: kadiatouaissatou@lenat.uganc.edu.gn, mohamedansoumane@lenat.uganc.edu.gn, boudal.niang@esmt.sn, sadigoudia@gmail.com, izdiakhate@gmail.com, souleymane@lenat.uganc.edu.gn

How to cite this paper: Barry, K.A., Camara, M.A., Niang, B., Diallo, M.S., Diakhaté, I. and Soumah, S. (2026) Comparative Analysis and Modeling of 4G LTE Propagation Using the Okumura-Hata and COST-231 Hata Models, Enhanced with Spatially Correlated Log-Normal Shadowing. *Journal of Electromagnetic Analysis and Applications*, **18**, 175-216.
https://doi.org/10.4236/jemaa.2026.1810010

Received: September 5, 2026
Accepted: September 25, 2026
Published: September 28, 2026

Abstract

Improving radio coverage and quality of service (QoS) is a major challenge for 4G LTE mobile networks, particularly in developing countries characterized by highly heterogeneous propagation environments. This study presents a comparative analysis of the Okumura-Hata and COST-231 Hata propagation models as applied to modeling the radio performance of 4G LTE networks. Both models were enhanced by incorporating spatially correlated log-normal shadowing to better represent the local fluctuations in the radio channel observed in real-world environments. The methodology adopted involves simulating propagation losses, received power, the signal-to-interference-plus-noise ratio (SINR), analytical coverage probabilities, and the performance of multicellular LTE networks in urban, suburban, and rural environments. Two-dimensional coverage maps were also generated to evaluate the spatial distribution of radio performance. Internal verification of the consistency of the simulations was performed using complementary statistical metrics, including RMSE, MAE, Pearson's correlation coefficient, the Nash-Sutcliffe index (NSE), and the Bland-Altman plot. The results show a gradual degradation in radio performance as obstacle density and interference levels increase. Rural environments generally offer more favorable propagation conditions, whereas urban environments impose greater constraints on LTE coverage and quality of service. A comparative analysis of the Okumura-Hata and COST-231 Hata models highlights the value of using them depending on the propagation conditions and frequencies under consideration. In the context of this study, the enhanced COST-231 Hata model appears, at first glance, to be a relevant approach for LTE networks operating at 1800 MHz, particularly due to its frequency range of application and the ability to incorporate corrections related to local propagation characteristics. However, its superiority over the Okumura-Hata model cannot be asserted in general terms and must be confirmed by experimental validation based on independent field measurements. Subject to this caveat, it constitutes a promising basis for the modeling and automatic optimization of LTE networks in Guinea.

Keywords

LTE-4G, Radio Propagation, Network Coverage, COST-231 Hata, Okumura-Hata, Shadowing, Guinea

1. Introduction

The 4G LTE mobile network is the radio technology that offers increased peak data rates (up to 50 Mbps and 100 Mbps for the uplink and downlink, respectively, at 20 MHz of bandwidth (BW)); and spectral efficiency (up to 2.5 bps/Hz and 5 bps/Hz for the uplink and downlink, respectively) [1]. In Guinea, as in many sub-Saharan African countries, the expansion of mobile networks has improved access to the Internet and digital services, thereby creating new economic and social opportunities [2]. Despite the expansion of mobile networks, Guinea faces persistent challenges regarding mobile network coverage and quality of service (QoS) [3]. A model of LTE network radio coverage, tailored to the Guinean context, is needed to better predict radio performance. Propagation models are commonly used in the planning of communication systems. They make it possible to predict signal coverage and calculate other parameters such as temporal dispersion or channel capacity [4]. They make it possible to measure the strength of the signal received by a mobile device, assess coverage areas, and determine the number of cells needed to cover a given area [5]. It also depends on the following factors: environments (urban, suburban, and rural), the distance between the transmitter (Tx) and receiver (Rx), operating frequency, atmospheric conditions, and altitude.

The objective of this article is to propose a mathematical framework that is both simple and rigorous, enabling the modeling of radio propagation, the estimation of RSRP, and the derivation of the associated geographic coverage. It also aims to compare the two proposed hybrid models by validating them using the MAE and RMSE error metrics, as well as radio quality expressed by the SINR, in order to identify the model best suited for future optimization mechanisms based on artificial intelligence. To provide a solid foundation for the modeling, this paper is organized as follows: the first section presents a general introduction; the second describes the modeling methodology adopted; and finally, the third section is devoted to the analysis and discussion of the results obtained.

A thorough analysis of the existing literature reveals that, to the best of our knowledge, no published academic study has specifically addressed the mathematical modeling of LTE propagation in Guinea. However, several studies conducted in various West African countries and other regions of the world address the modeling of LTE propagation using a variety of methodological and technical approaches. This literature review presents the main studies identified, along with their contributions and limitations.

The work by Noh Sun-Kuk and Choi Dong You (2019) proposed two LTE propagation models tailored for indoor and outdoor environments based on RSRP measurements. The results show better performance than the COST-231 model, with a prediction range of up to 400 m indoors and 200 m outdoors. However, the study is limited to urban microcellular environments and does not account for rural areas or 5G networks, with experiments restricted to a maximum speed of 120 km/h [6]. In the same context, Nuagah, Gadze-Dzisi, and Ahmed (2019) in Ghana studied improvements to LTE propagation models by comparing six models—namely SUI, ECC-33, Hata, COST-231, Free Space, and Ericsson—using MATLAB, artificial neural networks, and RMSE as the evaluation metric. The results showed that the Ericsson model performs best at 800 MHz in urban environments, while the SUI model is better suited for suburban areas. At 2.6 GHz, the ECC-33 model performed best. The authors also reduced prediction errors by applying the least-squares method. However, the study remains limited to six cities in Ghana and to urban and suburban environments [7]. In Nigeria, Nkordeh, Atayero, Idachaba, and Oni (2014), in their study titled "LTE Network Planning using the Hata-Okumura and the COST-231 Hata Pathloss Models", conducted a comparative analysis using MATLAB of the Okumura-Hata and COST-231 Hata models for LTE network planning. The results show that the Okumura-Hata model is better suited for low frequencies (150 - 1500 MHz), while the COST-231 Hata model offers better performance in dense urban environments between 1500 and 2000 MHz. The models were validated for distances ranging from 1 to 30 km and antenna heights between 30 and 200 m. However, the study is limited to simulations without experimental validation in the field [8]. In addition, Le Hachemi Mohammed Hicham (2017), in Algeria, studied the optimization of LTE/LTE-A network performance by analyzing the RSRP and SINR parameters using the VSS-LMS algorithm and the MATLAB simulator. The authors proposed two approaches for handover optimization: FSS-LMS for normal conditions and VSS-LMS for femtocell environments. The results show a significant improvement in performance compared to conventional methods. However, the study is limited to macrocell and femtocell environments, with no experimental validation or consideration of propagation models [9]. In Togo, Tossou Kodjo (2025) proposed an approach to optimizing the quality of service (QoS) of 4G networks based on modeling subscriber distribution, classifying areas of attractiveness, and generating traffic data in the absence of real-world data. The study uses combinatorial optimization methods and metaheuristics (greedy algorithm, tabu search, and genetic algorithms) for dynamic resource allocation and antenna configuration. The results indicate improvements in coverage, throughput, and traffic adaptability. However, this approach relies solely on simulated data and requires validation using field data to confirm its robustness. [10]. Finally, Stephen Jeswinde Nuagah, in collaboration with James Dzisi Gadze and Abdul-Rahman Ahmed (2019), in Ghana, also studied improvements to LTE propagation models. The results indicate that the Ericsson model offers the best performance at 800 MHz in urban environments, while the SUI model is better suited for suburban environments at the same frequency. At 2.6 GHz, the ECC-33 model proved to be the most effective. Furthermore, optimizing the models reduced the RMSE from 7.42 dB to 5.20 dB. However, the experiments were limited to six Ghanaian cities, and no validation was conducted in remote rural areas [11].

This literature review thus highlights the diversity of approaches used for modeling and optimizing LTE networks. However, it also reveals a lack of studies specific to the Guinean context, particularly with regard to rural, suburban, and urban environments, as well as the integration of real-world data from field measurement campaigns. This observation underscores the importance of the present research, which aims to propose a modeling approach adapted to the geographic and environmental realities of Guinea, using hybrid models such as Okumura-Hata + shadowing or COST-231 Hata + shadowing, tailored to the LTE frequencies used by telecommunications operators.

2. Methodology

The propagation loss model is an empirical mathematical formulation used to characterize the behavior of radio waves as a function of frequency, environment, and distance [12]. As part of this study, a MATLAB simulation was conducted to model radio wave propagation and coverage of 4G LTE networks in urban, suburban, and rural environments. To ensure that the results are representative and reliable, it is best to avoid using coefficients that are too high, as this could lead to an overestimation of propagation losses. Guinea exhibits significant geographic diversity (dense urban areas such as Conakry, the mountainous regions of Fouta-Djalon, the forested areas of Nzérékoré, and vast, sparsely urbanized rural areas). The coefficients must therefore remain consistent with the empirical propagation models used in 4G LTE networks. All of these parameters are presented in **Table 1** and **Table 2**.

Table 1. Simulation parameters.

Parameters	Okumura-Hata Values	COST-231-Hata Values
f	1800 MHz,	1800 MHz,
h_b	30 m	30 m
h_m	1.5 m	1.5 m
d	0.1 et 20 km	0.1 et 20 km

Continued

P_t	43 dBm	43 dBm
G_t	12 dBi	12 dBi
G_r	0 dBi	0 dBi
BW	20 MHz	20 MHz
L	0	0
Lm	3	3
Cm	-	3 (Urban), 0 (Suburban and Rural)
RSRP threshold	−105 dBm	−105 dBm
SINR_threshold	= −5 dB	= −5 dB
D_{corr}	20, 30, 50 m	20, 30, 50 m
Number of samples	500 sampling points	500 sampling points
Campsites	distances/locations/grid	distances/locations/grid

Table 2. Parameters for correcting for environmental factors.

Parameters	Values	Interpretations
K_vegetation	2 + 1.5 log10(d)dB	Correction Factors for dense vegetation
K_forest	+3 dB	Correction Factors for moderately dense vegetation
K_relief	+3 dB	Correction Factors for
K_climate	+2 dB	Correction Factors for Tropical humidity
K_infrastructure	−2 dB	Correction Factors for Low infrastructure density correction
$X\sigma$_urban	8 dB	Standard deviation of urban shadowing (dB)
$X\sigma$_suburban/ $X\sigma$_rural	6 dB	Standard deviation of rural/suburban shadowing (dB)

Guinea has a humid tropical climate, with annual rainfall that can exceed 4,000 mm in some regions [13]. Atmospheric humidity does not significantly affect the LTE bands between 1 and 2 GHz, but it can cause moderate additional losses. A correction of +2 dB appears reasonable. The expression 2 + 1.5log10(d) dB allows for modeling a gradual increase in losses as distance increases. As for terrain correction, a coefficient of +3 dB is sufficient to account for the topographical effects observed in mountainous regions without systematically overestimating losses across the entire country. Regarding shadowing, the proposed values are consistent with the literature on cellular networks; these values prevent an overestimation of shadowing that would artificially lead to a significant reduction in the coverage radius.

These parameters represent a good compromise between Guinea's specific environmental conditions and the values typically used in LTE modeling based on the Okumura-Hata and COST-231 Hata hybrid models with log-normal shadowing. They enable more realistic estimates of propagation loss, radio coverage, and quality-of-service indicators without introducing excessive model penalization.

2.1. Mathematical Modeling of Propagation

In mobile networks, the suitability of a propagation model depends on the specific site and is influenced by terrain obstacles, operating frequency, mobile device speed, sources of interference, and other constraints. Radio propagation is essential for emerging technologies, with design, deployment, and management strategies tailored to any wireless network. [14]. To minimize propagation losses during transmission, several path loss models have been proposed in the literature. In this study, two empirical propagation models are considered: the Okumura-Hata model and the COST-231-Hata model with shadowing.

These models are used to represent radio propagation conditions in urban, suburban, and rural environments. Comparisons between simulated values and synthetic reference data are considered in this study as an internal check of the consistency of the simulations and not as experimental validation or independent predictive validation. Indeed, since the reference data are generated numerically from the simulation framework, they do not constitute independent observations that can, on their own, establish the absolute accuracy or superiority of a propagation model. The RMSE, MAE, Pearson correlation coefficient, Nash-Sutcliffe index (NSE), and Bland-Altman plot are therefore used to characterize the internal consistency of the results obtained under the simulation conditions considered. External validation based on actual radio measurements taken in the field remains necessary to assess the generalizability of the proposed models.

2.1.1. Mathematical Modeling of the Okumura-Hata Model + Shadowing

1) The Okumura-Hata Model

The Okumura-Hata model is an empirical radio propagation model used to predict path loss in mobile networks in outdoor environments, such as urban, suburban, or rural areas. This model typically applies only to frequencies between 150 and 1,500 MHz, with base station antenna heights h_b (30 - 200 m) and mobile antenna heights h_m (1 - 10 m) [15]. The equation for the Okumura-Hata path loss model (PL_{OH}) is written as follows: [16]:

$$\begin{aligned} PL_{OH} = {} & 69.55 + 26.16\log_{10}(f) - 13.82\log_{10}(h_b) - a(h_m) \\ & + (44.9 - 6.55\log_{10}(h_b))\log_{10}(d) \end{aligned} \tag{1}$$

where:

- ✓ $PL_{OH}(d)$: Calculated path loss,
- ✓ 69.55: Empirical constant of the model for urban areas,
- ✓ f: Frequency of the LTE/3G/4G radio signal,
- ✓ $26.16\log_{10}(f)$: Decimal logarithm of the frequency,
- ✓ $13.82\log_{10}(h_b)$: Decimal logarithm of the base station height,
- ✓ h_b: Height of the base station antenna (BTS/eNodeB),

- ✓ h_m : Height of the mobile antenna (user),
- ✓ $a(h_m)$: Correction factor related to the mobile's height and the environment,
- ✓ *d*: Distance between the base station and the user,
- ✓ $\log_{10}(d)$: Decimal logarithm of the distance,
- ✓ $\left(44.9-6.55\log_{10}(h_b)\right)$: Factor representing the effect of distance and BTS height on attenuation.

2.1.2. Mathematical Modeling of the COST-231 Hata + Shadowing Model

1) COST-231 HATA Model

The COST-231 Hata model is widely used to calculate propagation losses in wireless mobile systems. The COST-231 Hata model is designed for use in the frequency band ranging from 500 MHz to 2000 MHz. It also includes corrections for urban, suburban, and rural (flat) environments [17]. The propagation loss of the COST-231 Hata model is calculated as follows [18]**:**

$$\begin{aligned} PL_{COST} &= 46.3+33.9\log_{10}(f)-13.82\log_{10}(h_b) \\ &\quad +\left(44.9-6.55\log_{10}(h_b)\right)\log_{10}(d)+C_m \end{aligned} \tag{2}$$

with:

- ✓ $C_m = 3$ dB in dense urban areas;
- ✓ $C_m = 0$ dB elsewhere.

where

- ✓ PL_{COST} : Calculated path loss;
- ✓ *f*: frequency in MHz;
- ✓ h_b: base station height (m);
- ✓ h_m: mobile height (m);
- ✓ $a(h_m)$: correction factor for the mobile;
- ✓ *d*: distance in km;
- ✓ C_m : terrain correction factor (0 dB for suburban areas, 3 dB for urban areas).

2.1.3. Correction Model for the Mobile Device

For urban, suburban, or rural areas, the correction factors related to the height of the receiver antenna are [19]:

- ➢ In urban areas for medium-sized or small cities:

$$a(hm)=\left(1.1\log(f)-0.7\right)hm-\left(1.56\log(f)-0.8\right) \tag{3}$$

- ➢ In urban areas for large cities, $f \geq 300$ MHz:

$$a(hm)=3.201\left(\log(11.75hm)\right)^2-4.97 \tag{4}$$

- ➢ In suburban areas:

$$L_{20}(\text{suburban})=L_{20}(\text{urban})-2\left(\log\left(\frac{f}{28}\right)^2\right)-5.4 \tag{5}$$

- ➢ In rural areas (open environment):

$$L_{20}(\text{rural})=L_{20}(\text{urban})-4.78\left(\log(f)\right)^2+18.33\log(f)-40.94 \tag{6}$$

2.1.4. Log-Normal Model

The log-normal propagation model is a generic model that extends the Friis model or the free-space model. It is used to predict propagation losses in a wide range of environments, whereas the Friis free-space model is limited to an unobstructed path between the transmitter and the receiver. The general form of the model is as follows [20]:

$$PL(d) = PL(d_0) + 10n\log 10\left(\frac{d}{d_0}\right) + Xdf \le d_0 \le d \tag{7}$$

where

- ✓ $PL(d)$: propagation loss at distance d(dB);
- ✓ $PL(d_0)$: loss at a reference distance (dB);
- ✓ n: propagation exponent (environment-dependent);
- ✓ d_0: reference distance (m);
- ✓ d: distance between the transmitter and the receiver (m, Km)

To account for the shading effect, a Gaussian random variable with a mean of zero and a standard deviation of $-\sigma$ is added to the equation [21].

Shading is modeled by a spatially correlated Gaussian process. The covariance between two positions d_i and d_j is defined by:

$$C(\Delta d) = \sigma^2 \exp\left(-\frac{|\Delta d|}{D_{corr}}\right) \tag{8}$$

with:

$$\Delta d = |d_i - d_j|$$

where:

- ✓ σ: represents the standard deviation of shadowing
- ✓ D_{corr}: the decorrelation distance.

Synthetic reference data is then generated according to:

$$P_{\text{ref}}(d_i) = P_{r,\text{model}}(d_i) + \epsilon_i, \tag{9}$$

with:

$$\epsilon_i \sim \mathcal{N}(0, \sigma_{\text{mes}}^2),$$

where:

- ✓ $P_{\text{ref}}(d_i)$: represents the synthetic reference data at point d_i;
- ✓ $P_{r,\text{model}}(d_i)$: represents the power received as calculated by the model;
- ✓ ϵ_i: is additive Gaussian noise;
- ✓ σ_{mes}: is the standard deviation of the synthetic reference data noise.
- ✓ $\epsilon_i \sim \mathcal{N}(0, \sigma^2)$: is the Gaussian random variable with a mean of zero.

In this context, this equation can be expanded to account for environmental factors:

$$PL_{Guinea} = PL + X_{\sigma,corr} + K_{climat} + K_{vegetation} + K_{relief} + K_{infra} \tag{10}$$

where:

- ✓ PL_{Guinea}: Total propagation loss in Guinea;

- ✓ PL : Propagation loss for the models;
- ✓ $X_{\sigma,corr}$: represents the log-normal shadowing;
- ✓ $K_{vegetation}$: correction factors for dense vegetation;
- ✓ K_{relief} : correction factors for mountainous terrain;
- ✓ K_{infra} : correction factors for low infrastructure density;
- ✓ K_{climat} : correction factors for tropical humidity.

2.1.5. Modeling the Received Signal Strength (RSRP)

RSRP (Reference Signal Received Power) represents the received power of the LTE signal. The received signal strength for the Okumura, Hat, and COST-231 models can be calculated as follows [22]:

$$P_r = P_t + G_t + G_r - PL_{predicts} - L \tag{11}$$

where:

- ✓ P_r : received power at the receiver (user's mobile device) (dBm);
- ✓ P_t : transmit power of the base station (eNodeB) (dBm);
- ✓ G_t : gain de l'antenne émettrice (dBi);
- ✓ G_r : Receiving antenna gain (phone/mobile) (dBi);
- ✓ $PL_{predicts}$: predicted total propagation loss (dB);
- ✓ L: loss at the connector and in the cable, in dB.

Estimated received power based on the link balance:

$$P_{r,model}\left(d\right) = P_t + G_t + G_r - PL\left(d\right) - X_\sigma\left(d\right) - L \tag{12}$$

where:

- ✓ $P_{r,model}\left(d_i\right)$: represents the estimated power received based on the link balance;
- ✓ σ_{mes} : is the standard deviation of the synthetic reference data noise;
- ✓ $X_\sigma\left(d\right)$: Correlated log-normal shadowing caused by natural and artificial obstacles (dB).

The Reference Signal Received Power (RSRP) is an essential indicator for assessing radio coverage and reception quality in LTE networks. In particular, it makes it possible to evaluate the power level of the signal received by the mobile terminal and to identify areas with satisfactory or degraded coverage. Thus, **Table 3** presents the thresholds used for RSRP classification.

Table 3. The RSRP power classification thresholds, as well as their interpretation in terms of LTE coverage quality [23].

RSRP Range (dBm)	Interpretation	Coverage Quality
RSRP ≥ −66	Excellent signal, very strong reception	Excellent
−94 ≤ RSRP ≤ −66,	Very good signal, strong coverage	Very good
−122 ≤ RSRP ≤ −94,	Average signal, general service	Acceptable
RSRP < −122	Weak signal, poor coverage	Bad

2.1.6. Modeling Radio Coverage

1) Multi-cell network

In a real network, multiple base stations contribute to the received signal; the mobile device connects to the cell that provides the best received signal strength. [24]. This approach makes it possible to map cell boundaries, overlapping areas, and radio shadow zones.

- **LTE coverage requirements**

Coverage and capacity requirements result in what are known as inequalities (signal-to-interference ratio), which must be satisfied for each user. These inequalities, which are at the heart of our model, take the following form [25]:

An area is considered covered only if:

- ✓ The received signal is strong enough:

$$P_r(x,y) \geq P_{\text{threshold}} \tag{13}$$

and

- ✓ the radio quality is adequate:

$$\text{SINR}(x,y) \geq \text{SINR}_{\text{threshold}} \tag{14}$$

Otherwise, the location is considered an area with poor coverage or a radio dead zone.

where:

- ✓ $P_r(x,y)$: Received signal power at point (x,y);
- ✓ $P_{\text{threshold}}$: Minimum acceptable received power threshold;
- ✓ SINR(x, y): Ratio of the received useful power to interference from other cells and thermal noise;
- ✓ $\text{SINR}_{\text{threshold}}$: Minimum acceptable SINR value.

- **Coverage radius**

This equation provides an estimate of the cell's maximum service radius.

$$d = d_0 \cdot 10^{\frac{P_t + G_t + G_r - L(d_0) - L_m - P_{\text{threshold}}}{10n}} \tag{15}$$

where:

- ✓ P_t: Transmission power of the base station (eNodeB) (dBm);
- ✓ G_t: Gain of the transmit antenna (dBi);
- ✓ G_r: Gain of the receive antenna (phone/mobile) (dBi);
- ✓ $L(d_0)$: Propagation loss at the reference distance d_0 (dB);
- ✓ L_m: Additional losses (cables, connectors, building penetration, vegetation, rain.) (dB);
- ✓ d: Maximum coverage distance (cell coverage radius) (Km ou m);
- ✓ do: Reference distance used to calculate propagation losses (m);
- ✓ $P_{\text{threshold}}$: Receiver sensitivity, *i.e.*, the minimum signal power required for proper reception (dBm);
- ✓ N: Path loss exponent, characterizing the rate of signal attenuation with distance.

- **Probability of coverage:**

This is the probability that the received power will exceed the minimum required threshold [26] [27]:

$$P_{\text{cov}} = P\left(P_r > P_{\text{threshold}}\right)$$
$$P_{\text{cov}} = Q\left(\frac{P_{\text{threshold}} - \overline{P}_r}{\sigma}\right) \quad (16)$$

where:

✓ P_{cov} : Coverage probability, *i.e.*, the probability that the received power exceeds the minimum required threshold (%);

✓ $P_{\text{threshold}}$: Minimum received power threshold guaranteeing successful communication (e.g., an RSRP threshold) (dBm);

✓ P_r : Power of the signal received by the user terminal (dBm);

✓ $P(\ )$: Probability function;

✓ $Q(\cdot)$: Q-function of the standard normal distribution, representing the probability that a standard normal random variable exceeds a given value;

✓ σ: Standard deviation of log-normal shadowing, representing signal fluctuations due to the environment.

➢ **Coverage rate**

This spatial coverage rate represents the proportion of the study area where the received power exceeds the required threshold [28]:

$$T_{\text{cov}} = \frac{\int_{\Omega} \mathbf{1}_{\left(P_r(x,y) \geq P_{\text{threshold}}\right)} \mathrm{d}\Omega}{\int_{\Omega} \mathrm{d}\Omega} \quad (17)$$

where:

✓ T_{cov} : Spatial coverage rate, representing the proportion of the study area where the received power exceeds the required threshold (%);

✓ $P_{\text{threshold}}$: Minimum received power threshold guaranteeing satisfactory communication (dBm);

✓ $P_r(x, y)$: Received power at the point with coordinates (x, y) (dBm);

✓ Ω: Study area or geographic region (coverage area) (m^2 ou km^2);

✓ $(P_r(x, y) \geq$ Pthreshold): Indicator function equal to 1 if the condition $P_r(x, y) \geq P_{\text{threshold}}$ is satisfied, and 0 otherwise;

✓ dΩ: Infinitesimal area element of the study area (m^2 ou km^2);

✓ $\int_{\Omega} \mathbf{1}_{\left(P_r(x,y) \geq P_{\text{threshold}}\right)} \mathrm{d}\Omega$: Area covered where the received power exceeds the threshold (m^2 ou km^2);

✓ $\int_{\Omega} \mathrm{d}\Omega$: Total area of the study area (m^2 ou km^2).

2.1.7. SINR Modeling (Radio Quality)

In 4G, performance depends in part on the signal-to-interference-plus-noise ratio (SINR), as shown in the following equations [29]:

$$\text{SINR} = \frac{S}{I + N} \quad (18)$$

Or in dB:

$$\text{SINR}_{\text{dB}} = P_r - 10\log 10\left(I + N\right) \quad (19)$$

With:

$$N = kTB \tag{20}$$

where:

- ✓ SINR: signal-to-interference-plus-noise ratio;
- ✓ S: useful signal;
- ✓ I: intercell interference;
- ✓ N: thermal noise;
- ✓ k: Boltzmann constant (1.3807×10^{-23} [J·k^{-1}]);
- ✓ T: absolute temperature (290˚k);
- ✓ B: bandwidth (20 MHz);
- ✓ SINR: signal-to-interference-plus-noise ratio in (dB) (The higher the SINR, the better the quality of the radio link);
- ✓ Pr: power of the signal received by the user from the base station (dBm) (The higher Pr, the better the coverage).

The Signal to Interference plus Noise Ratio (SINR) is a key indicator of radio link quality in LTE networks. Unlike the RSRP presented in **Table 3**, which mainly provides information on the received signal power level, **Table 4** shows the different SINR ranges and their corresponding radio link quality levels.

Table 4. The various SINR ranges and how they correspond to radio link quality levels, ranging from very poor to excellent [30].

SINR Interval (dB)	Interpretations	Radio Link Quality
SINR < −5	Very severe degradation, dominant interference	Very low
−5 - 0	A usable but unstable signal	Low
0 - 13	Service available but limited	Average
13 - 20	Generally reliable transmission	Good
SINR ≥ 20	Highly reliable connectivity, good 4G performance	Excellent

2.1.8. Model Validation

➢ **Root Mean Square Error (RMSE)**

The root means square error (RMSE) is commonly used as a standard statistical metric for evaluating model performance [31]. It is used to evaluate the error between field measurements and simulated values. The formula for RMSE is as follows [32]:

$$RMSE = \sqrt{\frac{1}{N}\sum_{i=1}^{N}\left(P_{ref,i} - P_{sim,i}\right)^2} \tag{21}$$

where:

- ✓ RMSE: Mean squared error between measured and predicted values
- ✓ N: Total number of measurement points;
- ✓ P_{ref}: power measured at point i;
- ✓ P_{sim}: power predicted/simulated by the model at point i.

➢ **Erreur absolue moyenne (MAE)**

MAE represents the average absolute difference between the simulation and the measurement. The lower the MAE, the better the accuracy. Equation (24) illustrates the calculation of the mean absolute error (MAE) [33] [34].

$$MAE = \frac{1}{n}\sum_{i=1}^{n}\left|y_i - \widehat{y_i}\right| \tag{22}$$

where:

- ✓ y_i : observed values at point i
- ✓ $\widehat{y_i}$: modeled values
- ✓ n: number of values

➢ **Pearson's correlation**

It measures the linear relationship between summary statistics and simulations. Pearson calls this method the "product moments" method. The formula can be expressed most simply as follows [35]:

$$r = \frac{\sum_{i=1}^{n}\left(y_i - \overline{y}\right)\left(\widehat{y_i} - \overline{\hat{y}}\right)}{\sqrt{\sum_{i=1}^{n}\left(y_i - \overline{y}\right)^2 \sum_{i=1}^{n}\left(\widehat{y_i} - \overline{\hat{y}}\right)^2}} \tag{23}$$

With:

$$-1 \le r \le 1$$

where:

- ✓ r: Pearson's correlation coefficient
- ✓ $\overline{y}$: mean of the measured values
- ✓ $\overline{\hat{y}}$: mean of the simulated values

➢ **Nash-Sutcliffe Efficiency Measure (NSE)**

The NSE (unitless) measures the relative magnitude of the residual variance (noise) compared to the variance of the fluxes (information); the optimal value is 1.0, and values must be greater than 0.0 to indicate a minimally acceptable performance. It is widely used for validating physical models. The equation is as follows [36]:

$$NSE = 1 - \frac{\sum_{i=1}^{n}\left(y_i - \widehat{y_i}\right)^2}{\sum_{i=1}^{n}\left(y_i - \overline{y}\right)^2} \tag{24}$$

where:

- ✓ NSE: Nash-Sutcliffe efficiency measure.

➢ **Bootstrap avec intervalle de confiance 95%**

Bootstrapping is a statistical method used to assign precision measures to statistical estimates. Typical values of B, the number of bootstrap samples, range from 50 to 200 for estimating the standard error. [37]. It (asymptotically) correctly estimates the variance of the sample median [38].

We generate B bootstrap samples:

Random draws with rebuys:

$$D_1^*, D_2^*, \cdots D_B^*$$

For each sample:

$$\theta_b^* = f\left(D_b^*\right) \tag{25}$$

The 95% confidence interval:

$$IC_{95\%} = \left[P_{2.5}\left(\theta^*\right), P_{97.5}\left(\theta^*\right)\right] \tag{26}$$

where:

✓ $P_{2.5}$: 2.5th percentile

✓ $P_{97.5}$: 97.5th percentile

Now, let's analyze and compare the two hybrid models-Okumura-Hata and COST-231—using spatially correlated log-normal shadowing, a multicellular model, environmental corrections tailored to the Guinean context, and statistical validation.

3. Results and Discussion

3.1. Analysis of the Okumura-Hata Method Using Shadowing

3.1.1. Analysis of Propagation Loss Using the Okumura-Hata Model

Figure 1 shows how propagation loss varies with distance in urban, suburban, and rural environments. This increase reflects the gradual attenuation of the radio signal as it propagates between the base station and the user equipment.

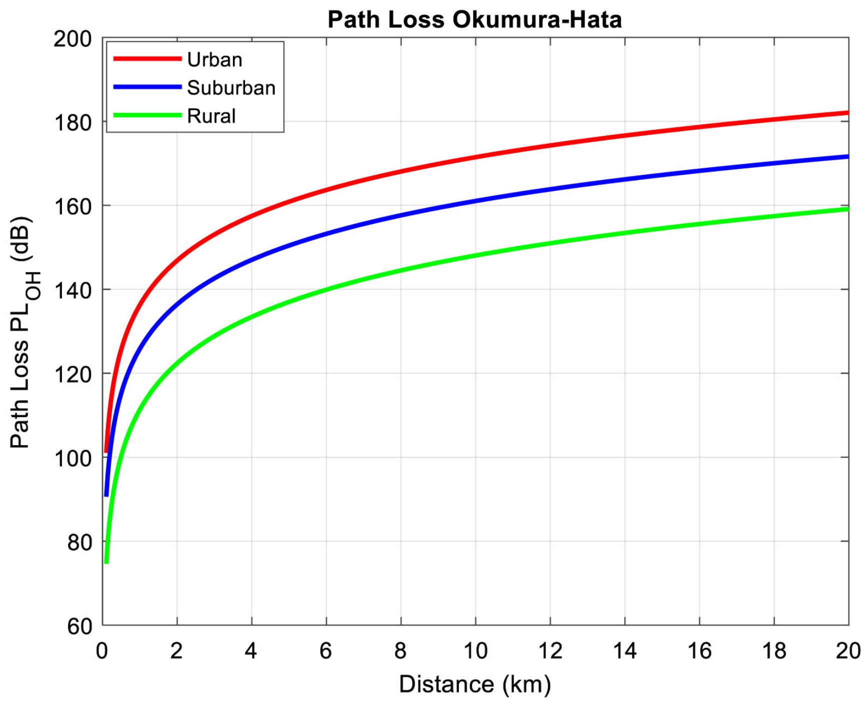

Figure 1. Propagation loss in the Okumura-Hata model.

The results in Figure 1 show that the urban environment experiences the greatest signal losses, a direct consequence of the high density of obstacles (buildings, infrastructure, and multiple reflections) that further degrade the propagation of radio waves. Conversely, the rural environment exhibits the lowest losses due to a lower density of obstacles, despite the inclusion of corrections for tropical climate, terrain, and vegetation. Suburban environments exhibit intermediate performance. These observations confirm that geographic characteristics significantly influence the radio performance of LTE networks. They also justify the use of propagation parameters specific to each environment in the context of mobile network optimization.

3.1.2. Effect of Log-Normal Shadowing on Propagation

Figure 2 illustrates the total propagation loss after accounting for spatially correlated log-normal shadowing. Unlike the previous theoretical curves, the observed fluctuations reflect the random variations caused by physical phenomena encountered in real-world networks (shadowing by buildings, vegetation, terrain, or user mobility).

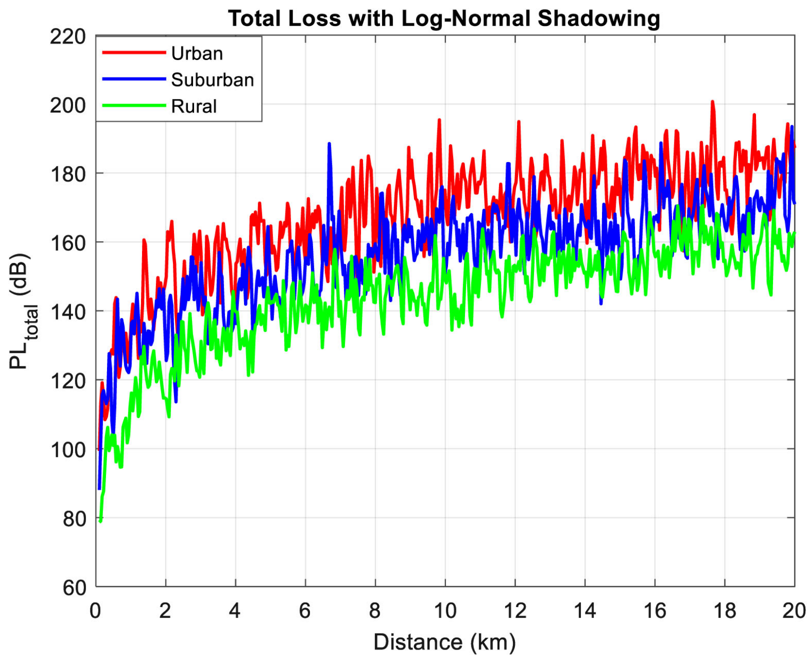

Figure 2. Total propagation loss due to shadowing.

The results in **Figure 2** also show that fluctuations are greater in urban environments ($\sigma = 8$ dB) than in suburban and rural areas ($\sigma = 6$ dB), reflecting greater variability in propagation conditions in heavily urbanized areas. These results indicate that this figure is more realistic than the previous one because it better reflects actual propagation conditions in a non-homogeneous environment.

3.1.3. Analysis of the Estimated Received Power Based on the Link Budget

Figure 3 shows the variation in LTE received signal strength as a function of distance, while incorporating the quality thresholds used in LTE networks as defined in the specifications of mobile network operators in Guinea; see **Table 3**.

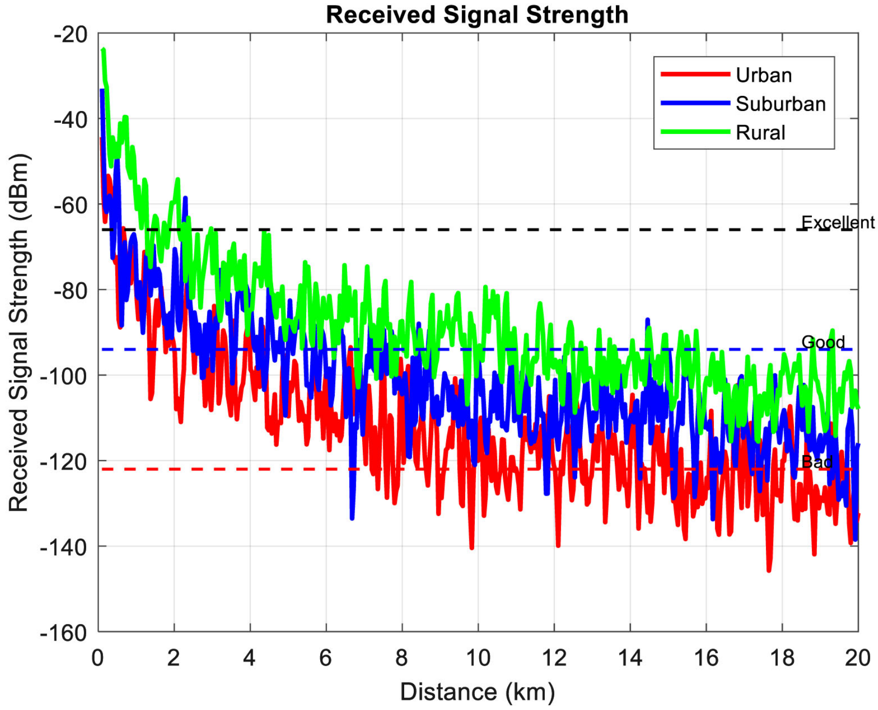

Figure 3. Received signal strength.

The results in **Figure 3** show a gradual decrease in Received Signal Strength as distance increases. This trend is consistent with the fundamental principles of radio propagation. Rural areas maintain higher power levels compared to urban areas due to lower propagation losses. Analysis of the LTE thresholds highlights three distinct regions: excellent radio coverage, acceptable service quality, and significant degradation of radio performance. The results indicate that received power remains highly dependent on environmental conditions. Urban areas reach acceptable coverage limits more quickly than suburban and rural areas, underscoring the need for a higher density of base stations in large metropolitan areas.

3.1.4. Signal-to-Interference-Plus-Noise (SINR) Analysis

Figure 4 shows the evolution of the signal-to-interference-plus-noise ratio (SINR) for the three environments studied.

Figure 4 shows a gradual decrease in SINR with distance, resulting from both the attenuation of the desired signal and the presence of intercellular interference. The urban environment remains the most susceptible to interference, as it was modeled at a level higher than thermal noise (+3 dB), unlike suburban (−3 dB) and rural (−5 dB) environments. The comparative analysis also shows that rural areas are better able to maintain a SINR above the minimum LTE threshold (−5 dB), thereby ensuring more robust radio communications. These results confirm that radio quality depends on both coverage and interference levels, justifying the combined use of RSRP and SINR metrics for evaluating LTE performance.

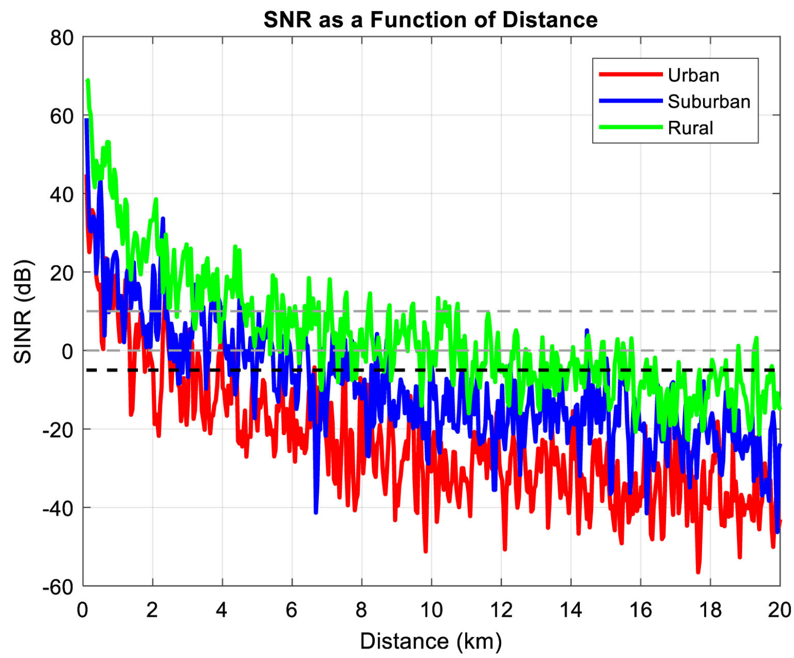

Figure 4. SINR as a function of distance for the Okumura-Hata Model.

3.1.5. Analytical Coverage Probability of the Okumura-Hata Model

Figure 5 shows the analytical coverage probability calculated based on the statistical properties of log-normal shadowing.

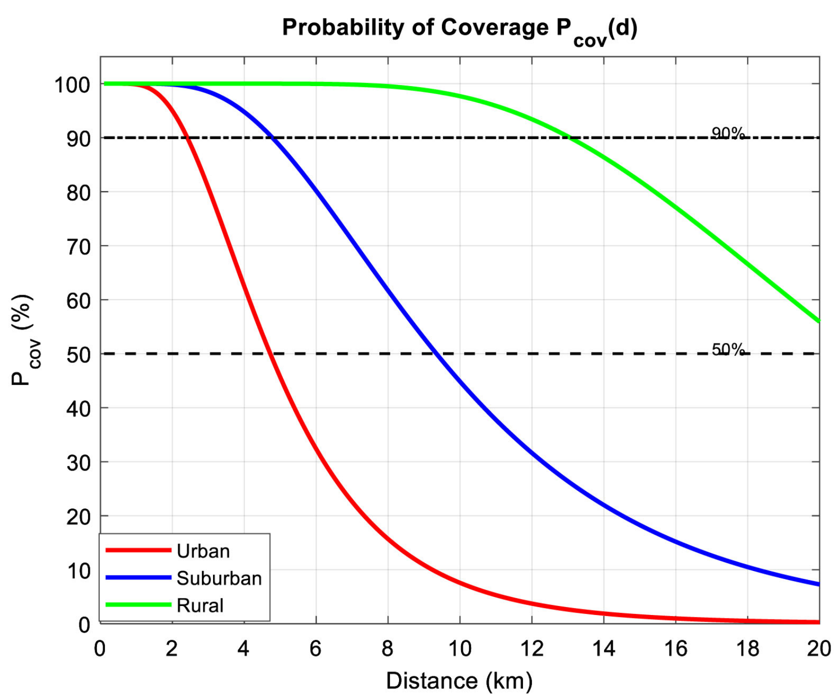

Figure 5. Probability of coverage.

The curves shown in **Figure 5** highlight a gradual decrease in coverage probability as distance increases. Rural areas naturally have the highest coverage probabilities, while urban areas experience a more rapid decline. The 50% and 90% thresholds identify the minimum and optimal limits of radio coverage, respectively. A probability greater than 90% is generally a relevant target for ensuring good service quality in LTE networks. This probabilistic approach provides particularly relevant additional information, as it allows for the incorporation of the uncertainty inherent in radio propagation phenomena.

3.1.6. Analysis of Spatial Coverage Maps

Figure 6 shows two-dimensional coverage maps of urban and rural areas, in which red indicates strong signal strength, yellow indicates good signal strength, green indicates fairly good signal strength, and blue and black indicate weak signal strength; white represents the coverage boundary.

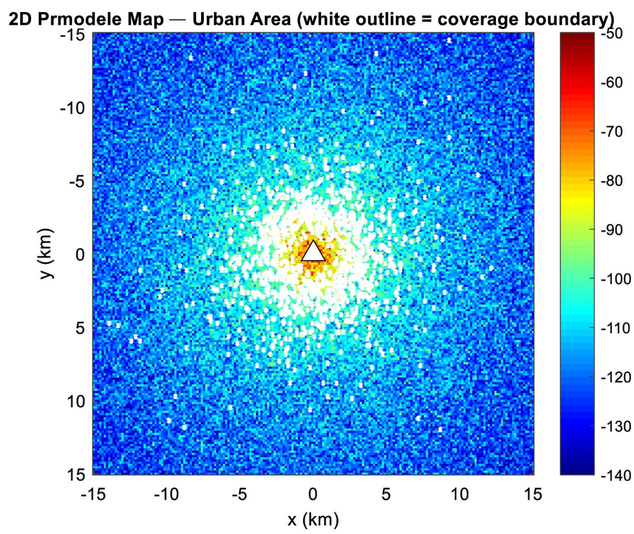

(a) Urban

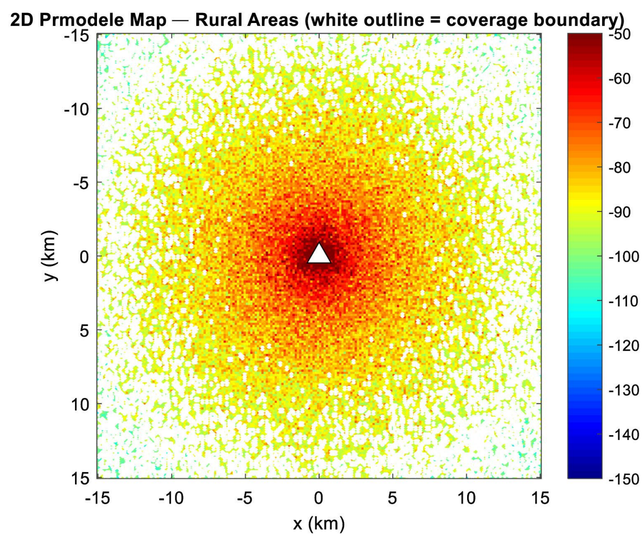

(b) Rural

Figure 6. Maps of estimated received power based on the 2D link budget (Okumura-Hata Model).

An analysis of **Figure 6** highlights the influence of shadowing phenomena on the spatial homogeneity of coverage. Rural areas exhibit larger and more homogeneous coverage zones than urban areas. This behavior is primarily due to lower propagation losses and reduced interference levels. These results demonstrate the value of spatial representations for identifying areas with potentially poor coverage that may require radio optimization.

3.1.7. Performance Analysis of a Multi-Cell Network

Figure 7(a) shows the spatial distribution of the SINR in a network consisting of seven base stations arranged in a simplified hexagonal architecture, while Figure b illustrates the dynamic assignment of users to the base station offering the best received power, as estimated from the link budget.

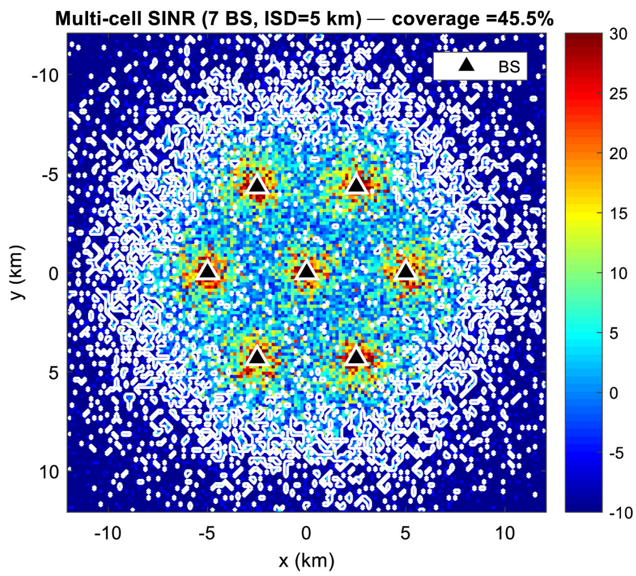

(a) Multi-cell SINR

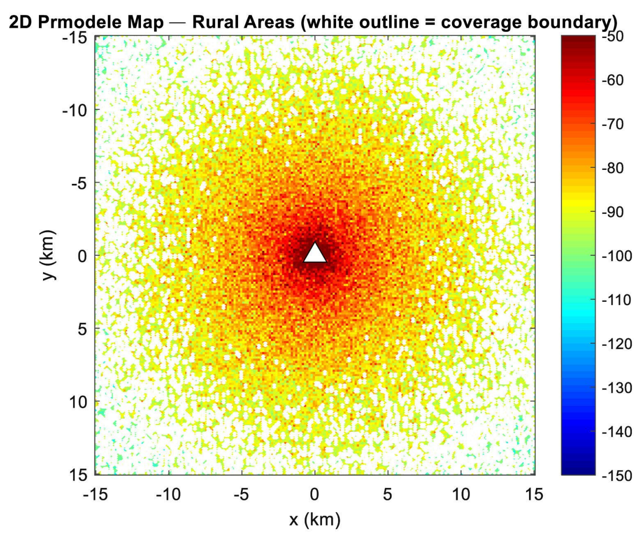

(b) BS (Voronoi) association

Figure 7. Multi-cell network performance (Okumura-Hata Model).

The results presented in **Figure 7** highlight the combined influence of inter-cell interference, user association mechanisms, and radio design parameters on the overall performance of the LTE network. The achieved multi-cell coverage is estimated at 45.5%, reflecting a degradation in performance in certain areas located primarily at cell boundaries where interference is more pronounced. These regions constitute critical areas that can simultaneously affect both the received power and the perceived radio quality experienced by users.

However, dynamically assigning users to the base station offering the best received power level improves local radio performance by optimizing the use of available resources. The results obtained nevertheless show that coverage improvement depends not only on the number of deployed base stations, but also on the selected radio parameters such as transmit power, inter-site distance, antenna tilt, and interference management mechanisms. These observations highlight the value of self-organizing network (SON) techniques for simultaneously improving coverage and quality of service in LTE networks.

3.1.8. Comparative Analysis of Propagation Media

Figure 8 presents a comparative summary of the average RSRP and SINR values obtained in the three environments studied.

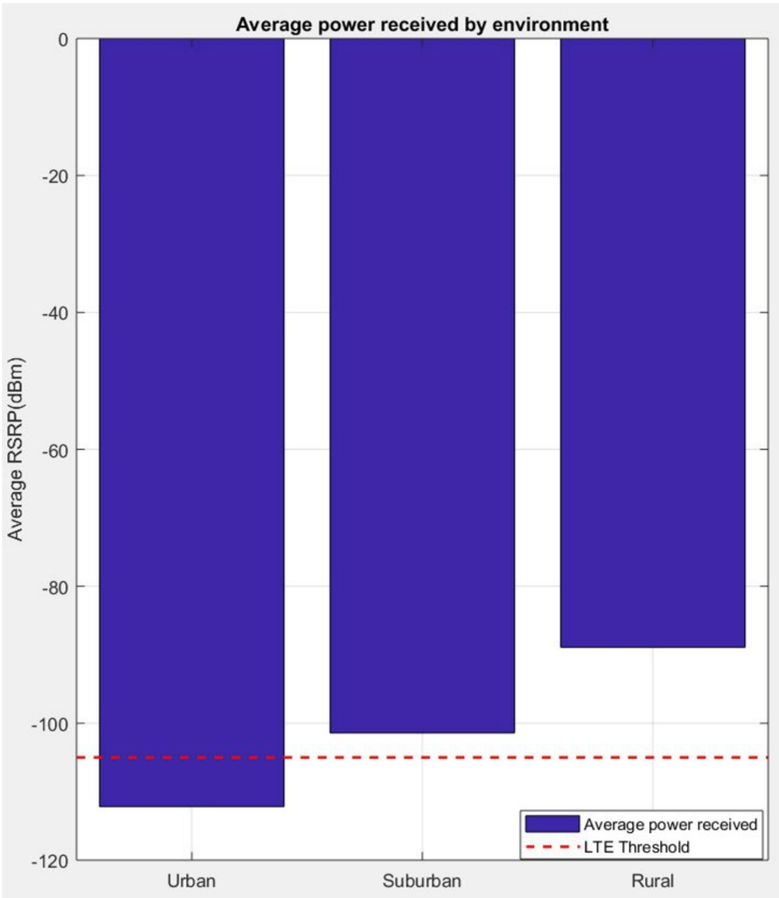

(a) Average power received by environment

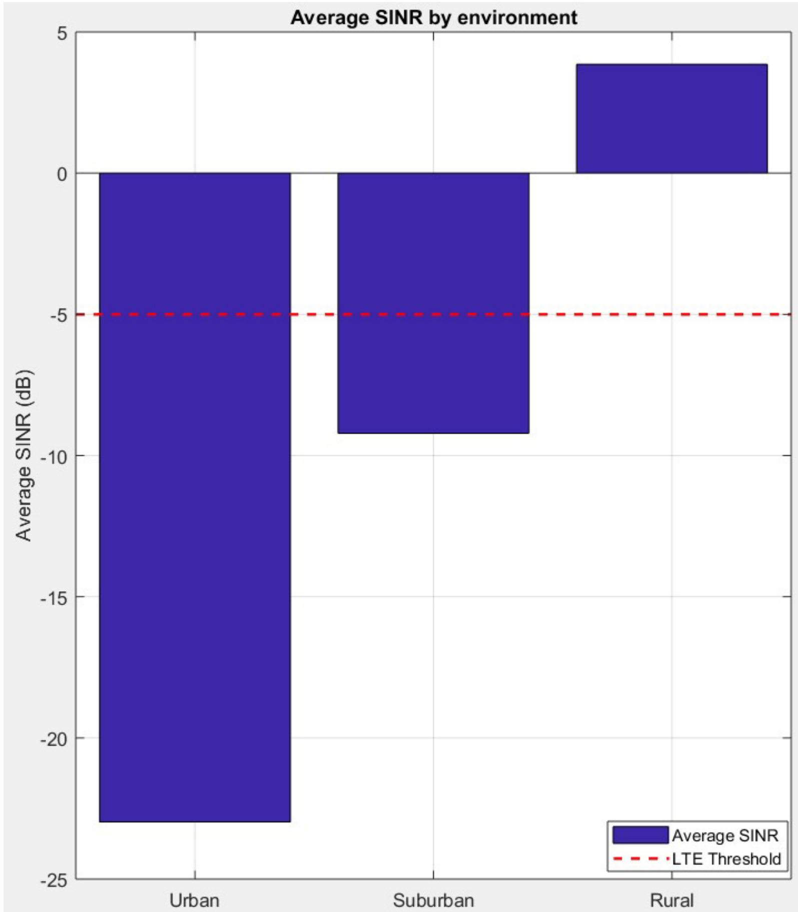

(b) Average SINR by environment

Figure 8. Comparative analysis of propagation media.

An analysis of **Figure 8** shows that radio performance generally decreases in the following order: Rural, Suburban, and Urban. The observed average values remain above the minimum LTE thresholds, reflecting the overall effectiveness of the proposed model in ensuring satisfactory coverage. This summary representation allows for the rapid identification of environments requiring greater optimization efforts when designing future mobile networks.

3.1.9. Validation of Simulations Using Synthetic Measurements for the Okumura-Hata Model

Figure 9 compares the simulation results with the synthetic reference data generated for each of the environments studied.

The results in **Figure 9** show strong agreement between the simulation predictions and the synthetic reference data generated for the three environments. The low RMSE values observed (1.91 dB in urban areas, 2.07 dB in suburban areas, and 2.14 dB in rural areas) indicate good internal consistency between the simulated results and the synthetic reference data generated under the conditions considered. However, they do not constitute an independent predictive validation of the model, as this requires experimental field measurements.

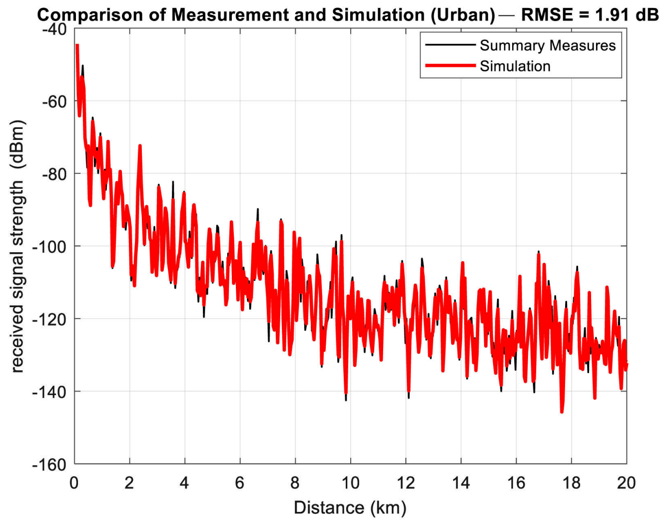

(a) Urban

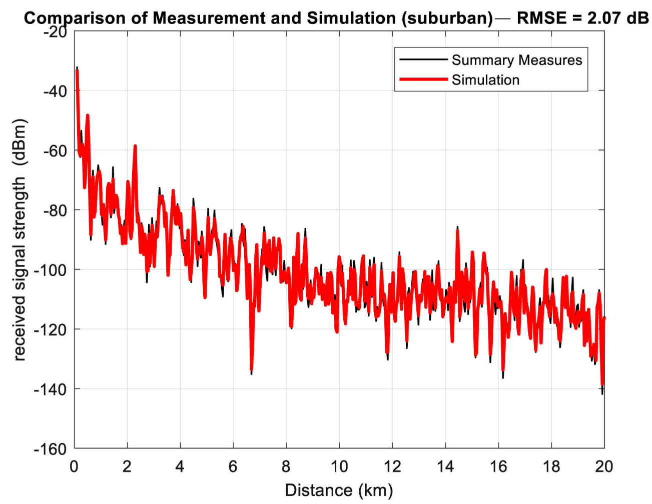

(b) Suburban

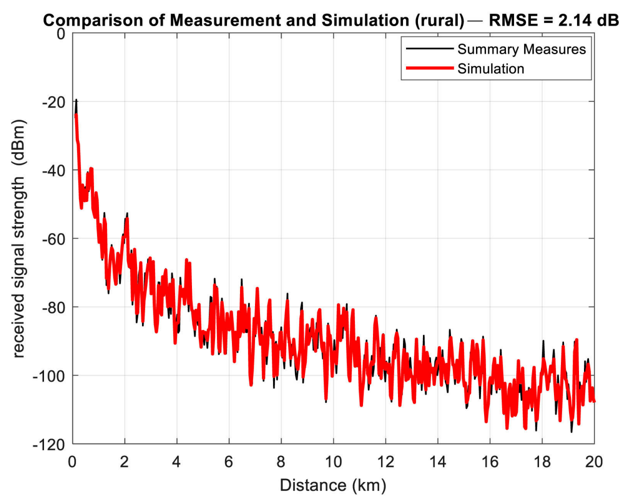

(c) Rural

Figure 9. Comparison of simulations with generated synthetic reference data (Okumura-Hata Model).

3.1.10. Statistical Validation of the Model

Several complementary statistical indicators were used to assess the robustness of the proposed model.

- **Pearson's correlation**

Figure 10 shows the relationship between the synthetic reference data and the simulations. Pearson's correlation coefficient is close to 1, indicating excellent agreement, and the p-value is < 0.05, indicating a statistically significant relationship.

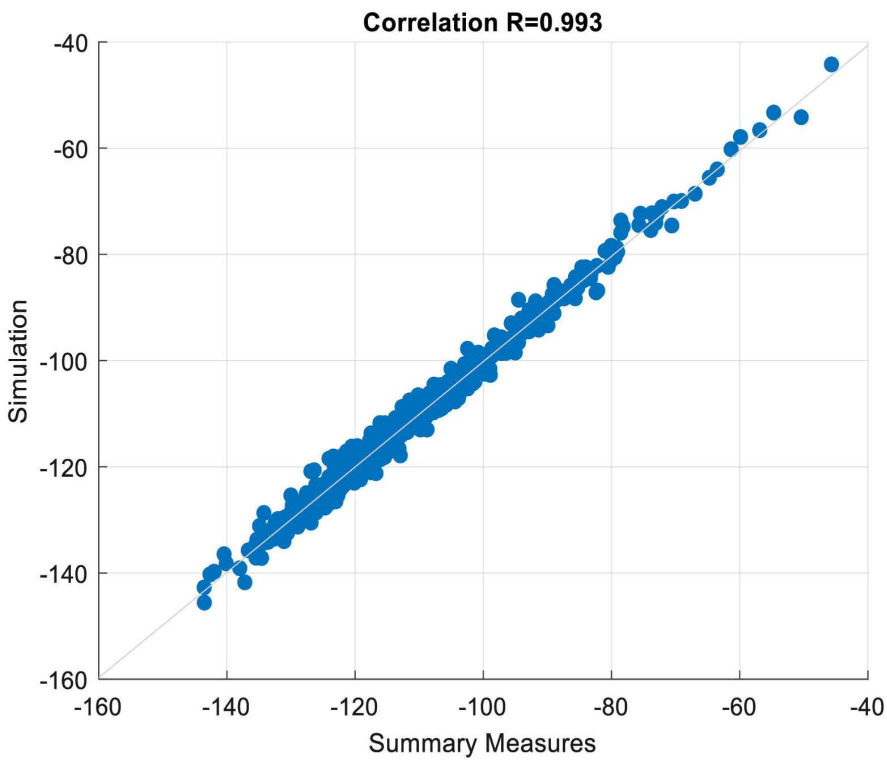

Figure 10. Pearson's correlation coefficient.

Analysis of Figure 10 shows a correlation coefficient that is substantially equal to 1; this result indicates a strong linear relationship between the synthetic reference data and the predictions obtained through simulation. This statistical validation reinforces the descriptive quality of the proposed model.

- **Bland-Altman plot**

Figure 11 shows the Bland-Altman plot, which assesses the agreement between the synthetic reference data and the simulations. Three lines are plotted: the mean bias, the upper limit ($+1.96\sigma$), and the lower limit (-1.96σ).

The results in Figure 11 show that the majority of the data points (samples) remain concentrated around the mean bias-hat is, between the upper and lower limits of σ. This not only indicates agreement between the synthetic reference data and the simulations but also serves as a positive indicator of the statistical validity of the proposed model.

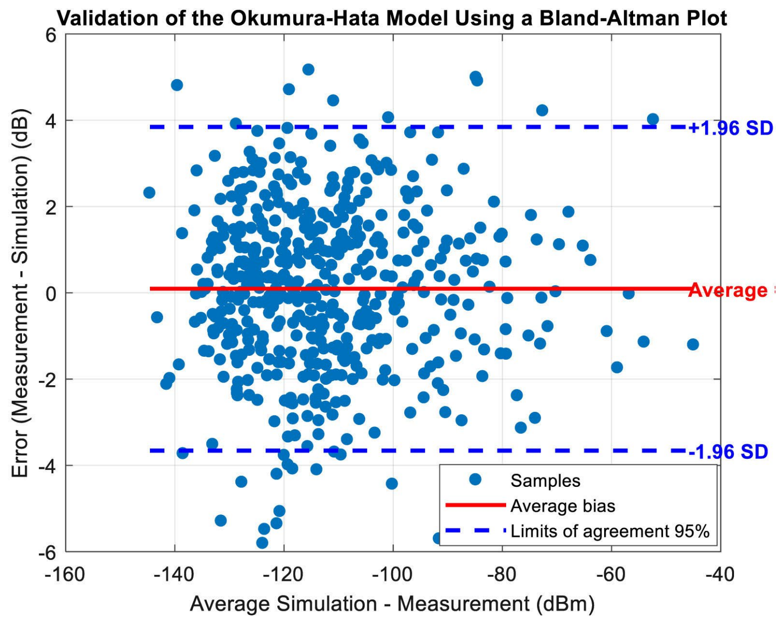

Figure 11. Bland-Altman plot for the Okumura-Hata Model.

Correlation

Pearson R = 0.9933 (p = 0.00000)

MAE = 1.52 dB

NSE = 0.9867

The Pearson correlation coefficient obtained (R = 0.9933; $p < 0.05$) indicates a very strong linear relationship between the synthetic reference data and the simulated values. This statistically significant correlation reflects the model's ability to accurately reproduce the observed variations in received power levels. Furthermore, the low MAE value (1.52 dB) indicates that the mean absolute errors in prediction remain limited, while the Nash-Sutcliffe index (NSE = 0.9867) confirms the excellent consistency between the observations and the simulations. The results of the Bland-Altman plot reveal a very low mean bias (0.09 dB) associated with relatively narrow limits of agreement (−3.66 dB; +3.85 dB), indicating good statistical stability of the predictions obtained. Taken together, these statistical indicators demonstrate the internal robustness of the proposed model and its ability to reproduce the propagation phenomena considered in this study. However, this validation is still based on synthetic reference data and will need to be corroborated by in-the-field radio measurements.

Let us now analyze the COST-231 Hata model adapted to LTE frequencies around 1800 MHz, incorporating spatially correlated log-normal shadowing, a multicell model, environmental corrections tailored to the Guinean context, and a comprehensive statistical validation of the radio predictions.

3.2. Analysis of the COST-231 Hata Model with Shadowing

3.2.1. Analysis of Propagation Loss Using the COST-231 Hata Model

Figure 12 shows the variation in propagation loss obtained from the COST-231

Hata model in urban, suburban, and rural environments. Although both the Okumura-Hata and COST-231 Hata models were evaluated at a frequency of 1800 MHz, the COST-231 Hata model is particularly well-suited for modeling LTE networks operating in this frequency band. This choice thus reinforces its relevance for analyzing the coverage and quality of service of the 4G networks considered in this study.

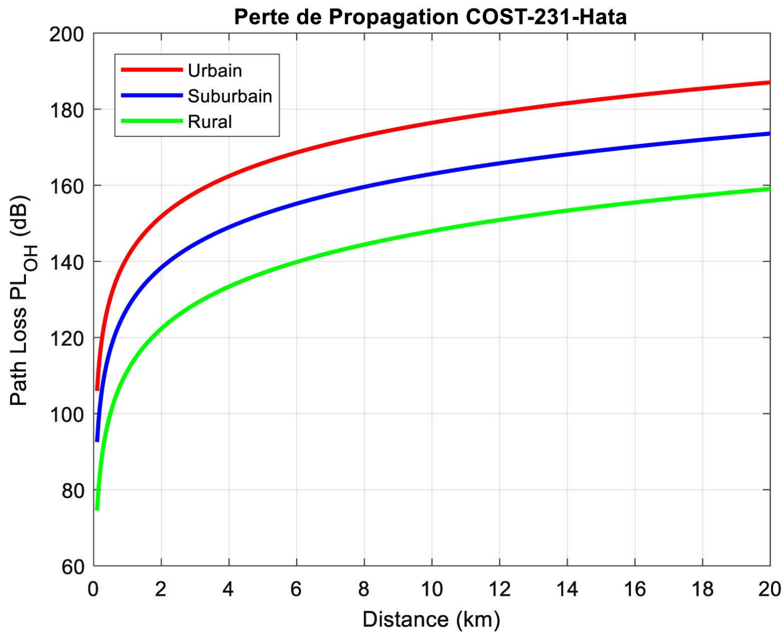

Figure 12. Propagation loss cost-231.

The results in **Figure 12** show a logarithmic increase in propagation loss with distance, consistent with empirical radio propagation models. The dense urban environment exhibits the highest losses due to the combined effects of infrastructure density, diffraction, and multiple reflections of electromagnetic waves. Suburban and rural environments exhibit lower losses after applying specific corrections related to the tropical climate, vegetation, and terrain. These observations highlight the significant influence of environmental characteristics on the performance of LTE networks and justify the introduction of the proposed corrective parameters for the Guinean context.

3.2.2. Effect of Spatially Correlated Log-Normal Shadowing

Figure 13 illustrates the effect of log-normal shadowing on the total propagation loss. The inclusion of spatially correlated shadowing represents a significant improvement to the model, as it allows for the reproduction of the local fluctuations observed in real-world radio environments.

The irregularities observed in **Figure 13** result from shadowing effects caused, in particular, by buildings, vegetation, or topographic variations found in the various regions studied. The standard deviations used (8 dB for urban areas versus 6 dB for suburban and rural areas) adequately reflect the greater variability of radio channels in heavily urbanized environments. The use of spatially correlated shadowing also improves the spatial consistency of radio predictions, a particularly important aspect in two-dimensional coverage analyses.

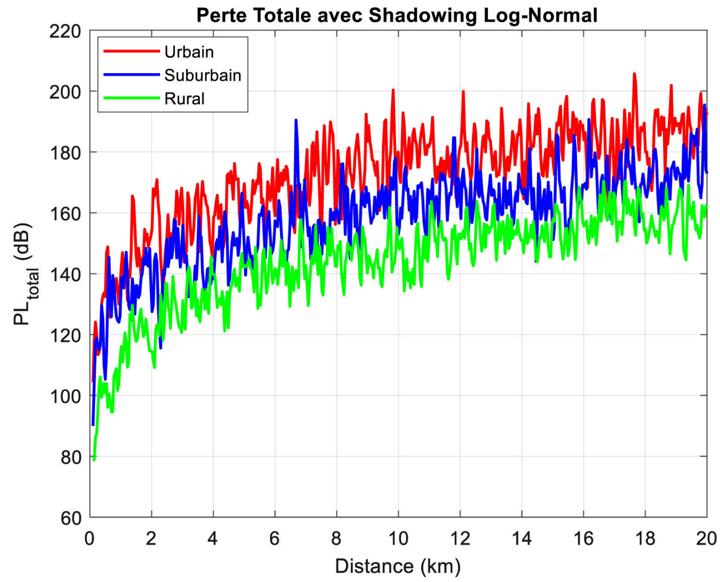

Figure 13. Total loss with shadowing.

3.2.3. Analysis of Radio Performance Based on Estimated Received Power Derived from the Link Budget

Figure 14 shows the variation in estimated received power, calculated from the LTE link budget, as a function of distance for the three environments studied.

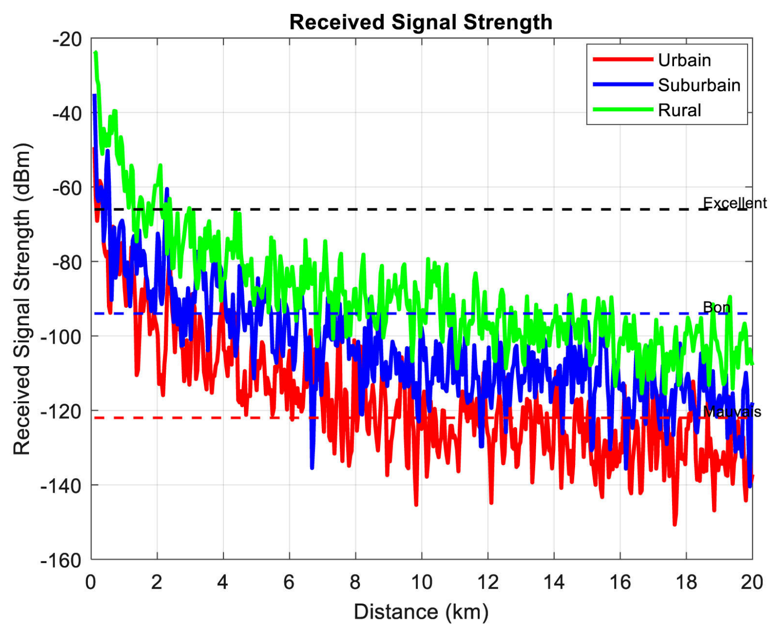

Figure 14. Estimated received power derived from the link budget.

The results shown in **Figure 14** indicate a gradual decrease in the received power level as the distance between the user and the base station increases. This degradation is directly related to the increase in propagation losses predicted by the COST-231 Hata model. Analysis of the various LTE thresholds indicates that rural areas maintain higher average received power levels estimated from the link budget than urban environments, thanks to more favorable propagation conditions. Conversely, urban environments reach critical radio coverage thresholds more quickly, underscoring the importance of cell sizing in densely populated areas. These results confirm that received power estimated from the link budget remains an essential indicator for evaluating LTE radio coverage, but that it must be combined with complementary radio quality indicators such as SINR.

3.2.4. Comparative Analysis of the SINR

Figure 15 shows how the signal-to-interference-plus-noise ratio (SINR) changes as a function of distance.

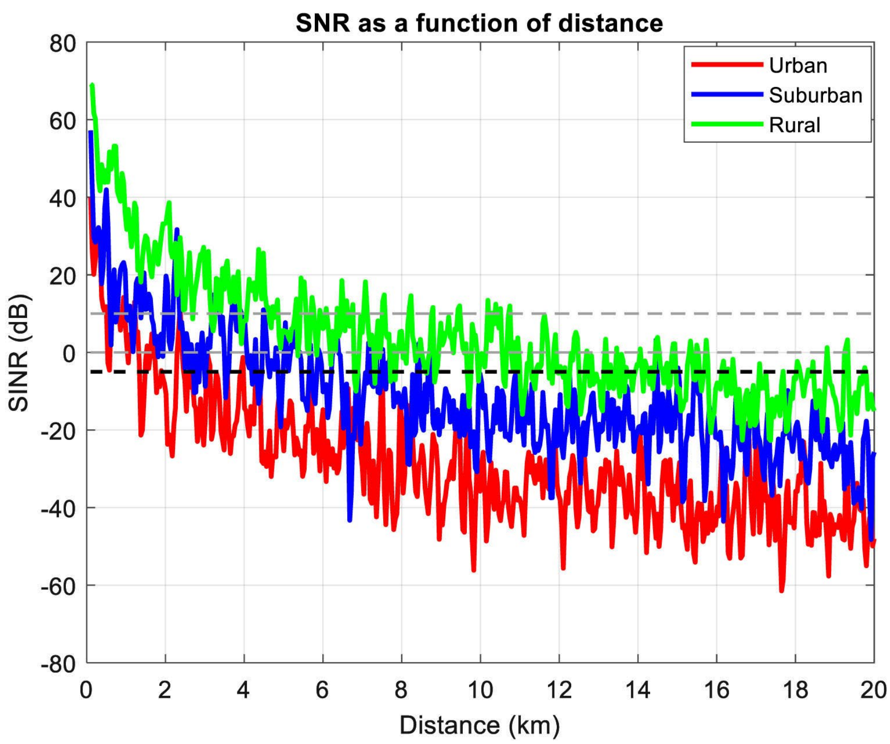

Figure 15. SINR as a function of distance for the COST-231 Hata Model.

The results in Figure 15 show that radio performance gradually decreases as distance increases due to the combined effect of signal attenuation and the relative increase in intercellular interference. Urban environments are naturally more susceptible to interference due to modeled interference levels that are +3 dB above thermal noise. Suburban and rural environments exhibit better performance due to lower interference levels. Maintaining a SINR above the minimum LTE threshold (−5 dB) is a particularly important indicator, as it directly determines the performance of the modulation and coding schemes used by the network. These observations confirm that satisfactory radio coverage does not automatically guarantee good quality of service. Simultaneous optimization of RSRP and SINR therefore remains essential when designing LTE networks.

3.2.5. Analytical Coverage Probability of the COST-231 Hata Model

Figure 16 shows the variation in the analytical coverage probability derived from the statistical properties of log-normal shadowing. The 50% and 90% thresholds identify the minimum and optimal LTE coverage limits, respectively.

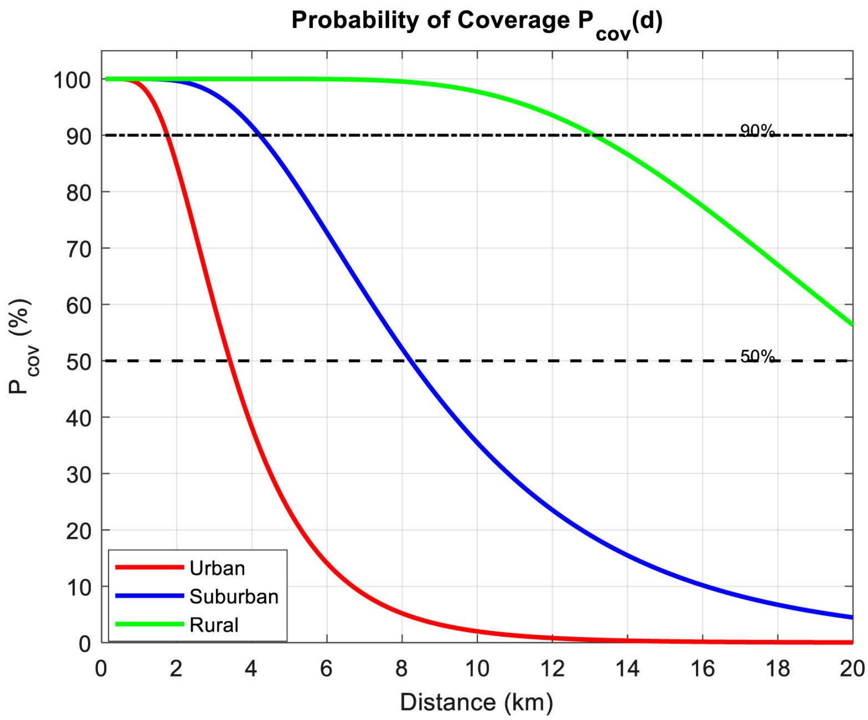

Figure 16. Coverage probability.

The results in Figure 16 show that the coverage probability gradually decreases with distance in all three environments studied. Rural areas naturally maintain the highest coverage probabilities due to their favorable propagation conditions, while urban environments exhibit a more rapid decline in radio performance. A probability greater than 90% is generally sought during radio optimization operations to ensure excellent quality of service for users. This probabilistic approach is a particularly relevant complement to deterministic analyses, as it allows for the explicit incorporation of the uncertainty inherent in radio propagation phenomena.

3.2.6. Spatial Analysis of Radio Coverage

Figure 17(a) and Figure 17(b) show the two-dimensional RSRP maps obtained in urban and rural environments, respectively. The white contours represent the coverage boundaries that simultaneously satisfy the constraints imposed on the RSRP and the SINR.

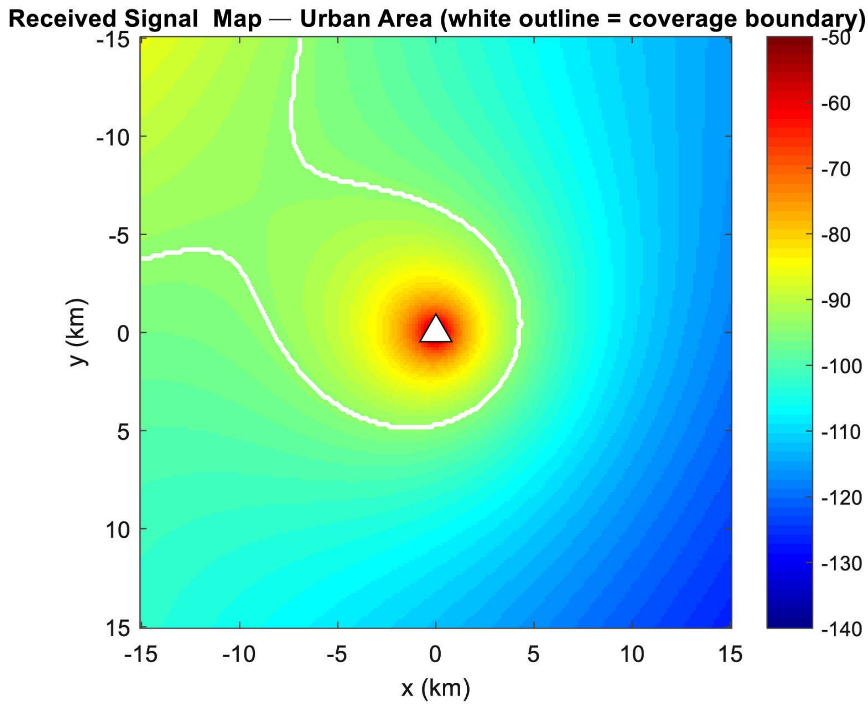

(a) Urban

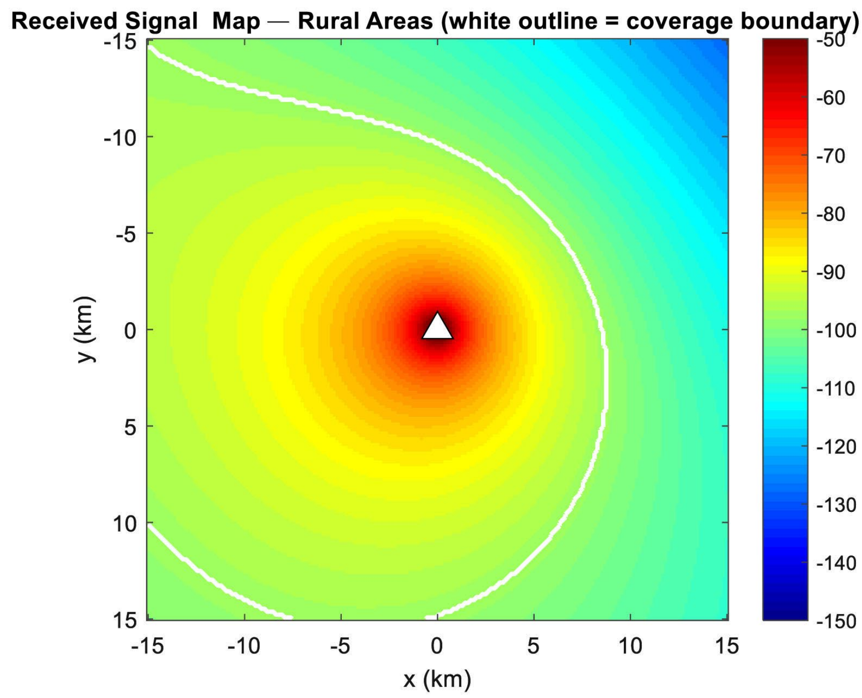

(b) Rural

Figure 17. Maps of estimated received power based on the 2D link budget (COST-231 Hata Model).

Figure 17(a) shows the spatial distribution of the SINR in a network consisting of seven base stations deployed in a simplified hexagonal architecture, while Figure 17(b) illustrates the mechanisms for dynamically associating users with the base station offering the highest received power level.

A visual analysis of **Figure 17** shows that rural areas have larger coverage areas and greater spatial homogeneity compared to urban areas. The fluctuations observed in the coverage maps result directly from the spatially correlated shadowing introduced into the simulations. This feature allows for a more accurate reproduction of the irregularities observed in real mobile networks. These results highlight the value of spatial analyses in identifying areas of poor coverage that may require radio optimization.

3.2.7. Analysis of the LTE Multicellular Network

The results presented in **Figure 18** show that, under the selected simulation conditions, the COST-231 Hata model yields a multicell coverage rate of 68.3%, which is higher than that obtained with the Okumura-Hata model (45.5%). However, this difference depends on the assumptions used to calculate coverage, the multicell geometry, the radio thresholds, and the environmental corrections applied. The spatial analysis of the SINR also shows that areas located at cell boundaries remain the most susceptible to intercellular interference. Despite these constraints, the performance achieved remains generally satisfactory in areas with actual coverage, thanks to dynamic user association mechanisms and improved spatial allocation of radio resources. These results underscore the value of multicellular architectures combined with modern optimization techniques for simultaneously improving radio coverage and quality of service in LTE networks.

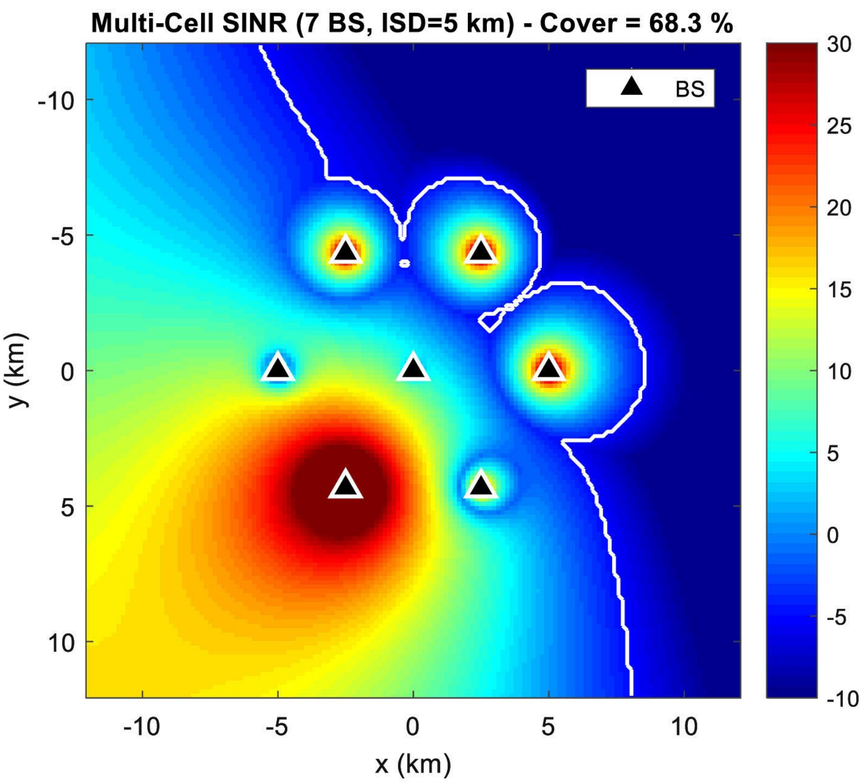

(a) Mult-cell SINR

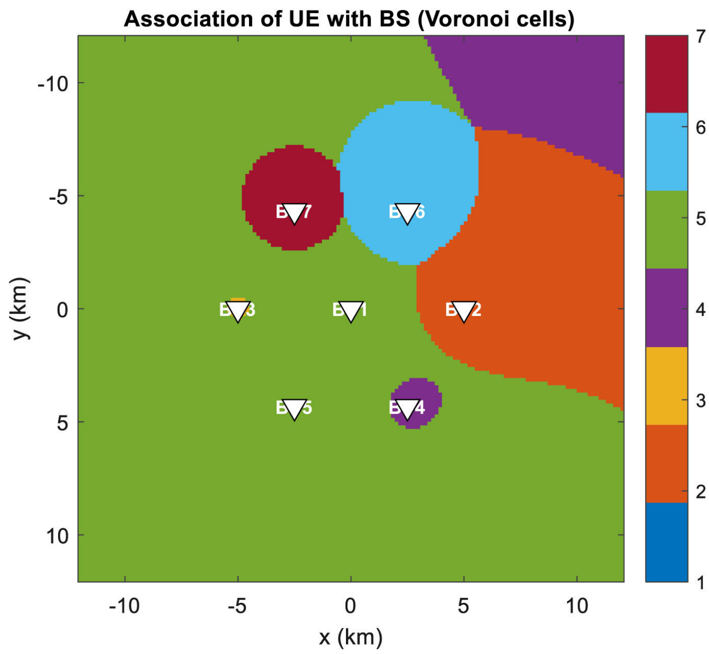

(b) Association of UE with BS

Figure 18. Multi-cell network performance (COST-231 Hata Model).

3.2.8. Comparative Analysis of Propagation Environments

Figure 19 presents a comparative summary of the average performance results obtained for RSRP and SINR in the three environments studied.

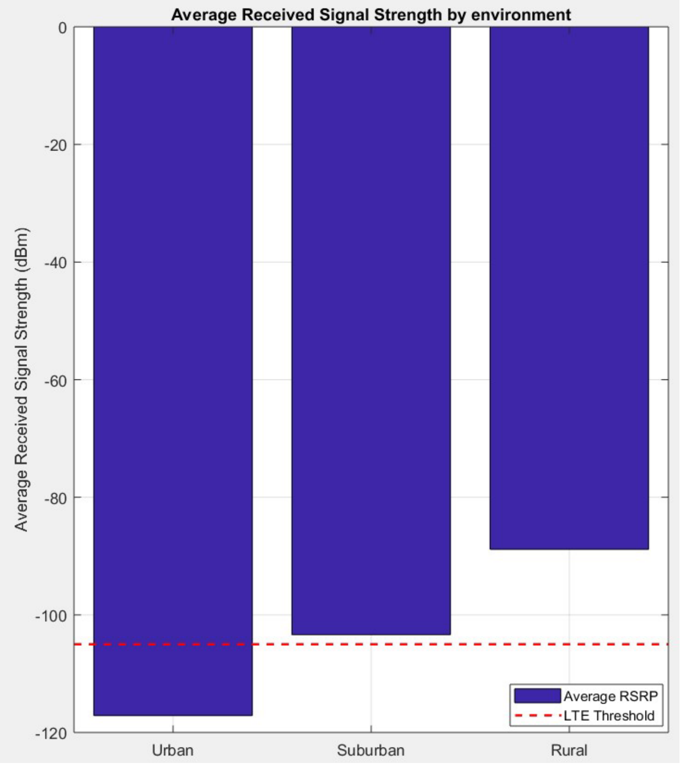

(a) Average power received by environment

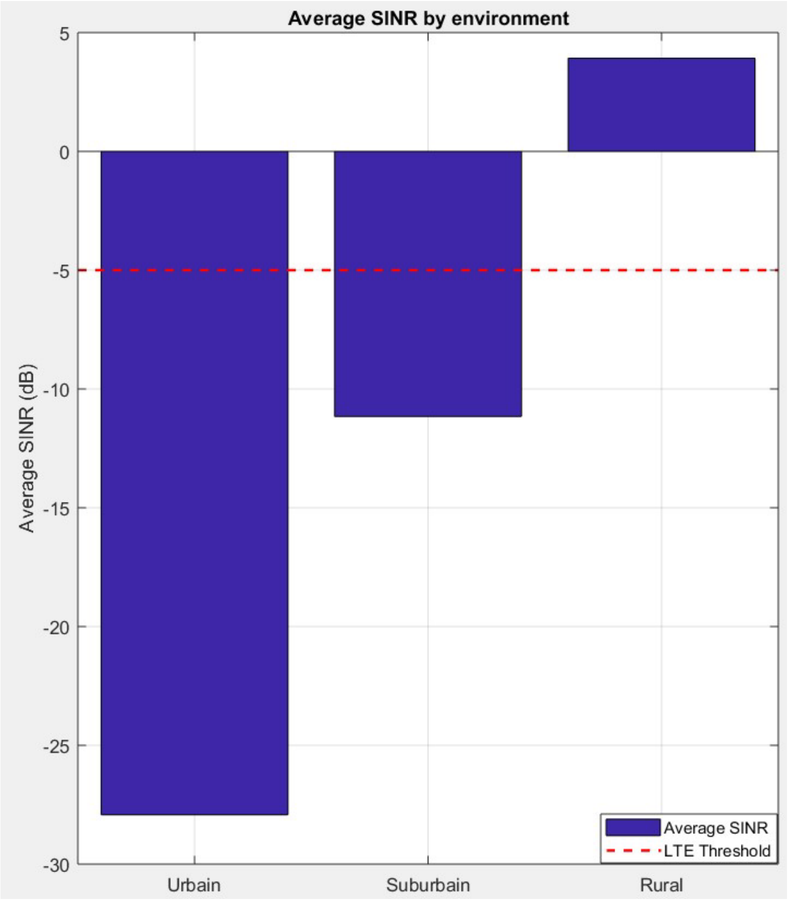

(b) Average SINR by environment

Figure 19. Comparative analysis of environments.

The results presented in **Figure 18** show that, under the selected simulation conditions, the COST-231 Hata model yields a multicell coverage rate of 68.3%, which is higher than that obtained with the Okumura-Hata model (45.5%). However, this difference depends on the assumptions used to calculate coverage, the multicell geometry, the radio thresholds, and the environmental corrections applied.

3.2.9. Validation of Simulations Using Synthetic Measurements for the COST-231 Hata Model

Figure 20 compares the simulation results with the synthetic reference data generated for each of the environments studied.

The results presented in **Figure 20** highlight a strong similarity between the synthetic reference data and the simulation results obtained in the three environments. The relatively low RMSE values observed (1.91 dB in urban areas, 2.07 dB in suburban areas, and 2.14 dB in rural areas) indicate good accuracy in the radio predictions obtained using the COST-231 Hata model enhanced with spatially correlated log-normal shadowing. The small discrepancies observed between the synthetic reference data and the simulations reflect the model's ability to reproduce the spatial variations of the radio channel while incorporating the combined effects of propagation phenomena, shadowing, and the proposed environmental corrections. These results are a positive indicator of the model's suitability for evaluating LTE radio performance at 1800 MHz in the environments under consideration.

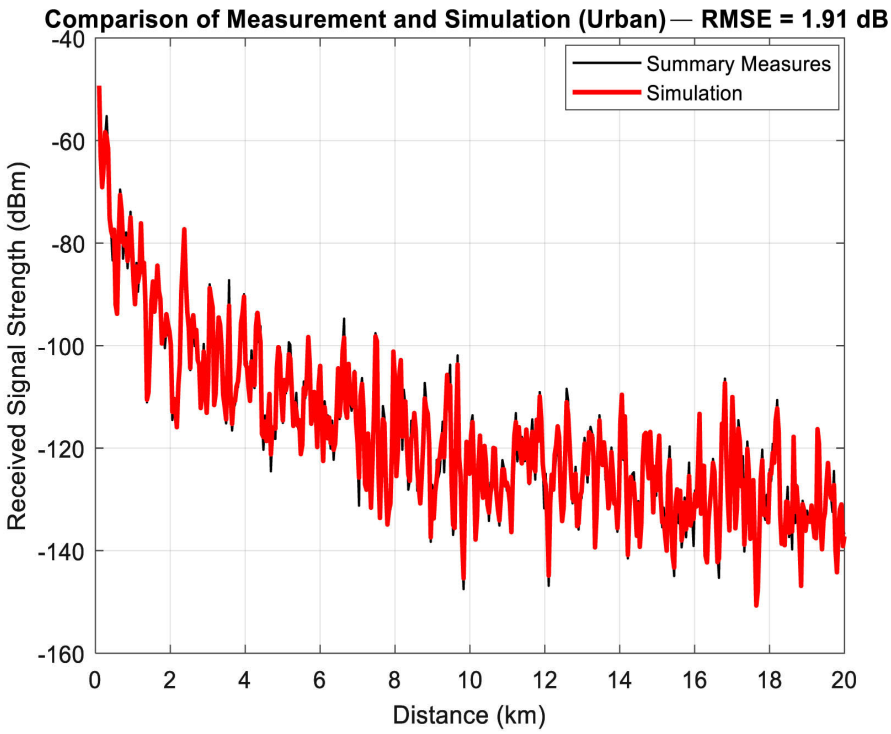

(a) Urban

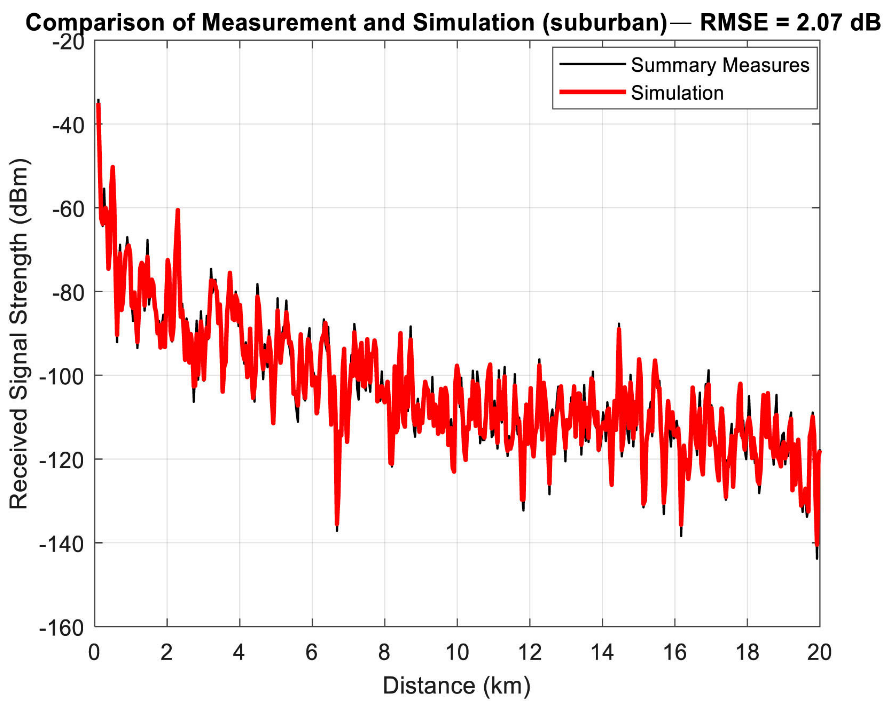

(b) Suburban

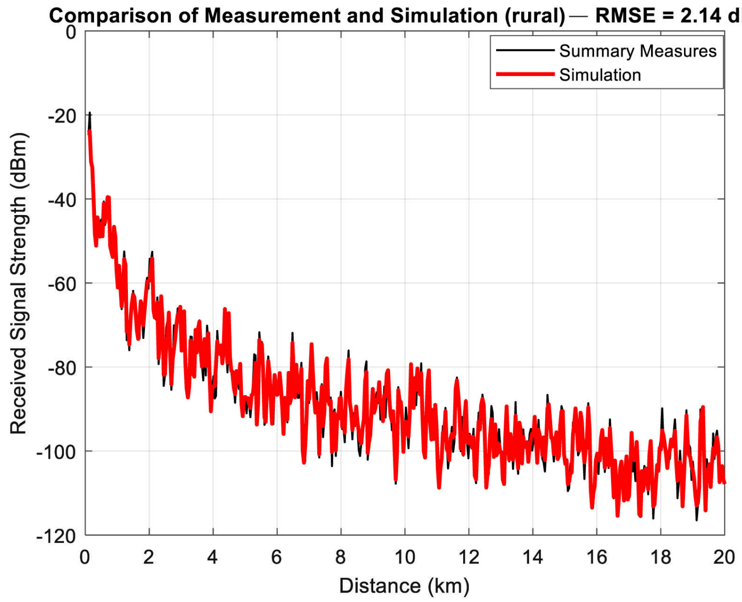

(c) Rural

Figure 20. Comparison of simulations with generated synthetic reference data (COST-231 Hata Model).

3.2.10. Statistical Validation of the COST-231 Hata Model

This model was statistically validated using several complementary metrics, namely: Pearson's correlation coefficient, mean absolute error (MAE), the Nash-Sutcliffe index (NSE), and the Bland-Altman plot. These metrics allow for an assessment of the internal consistency between the simulated results and the synthetic data generated under the conditions under consideration.

➢ **Pearson's correlation**

Figure 21 evaluates the relationship between the synthetic reference data and the simulations.

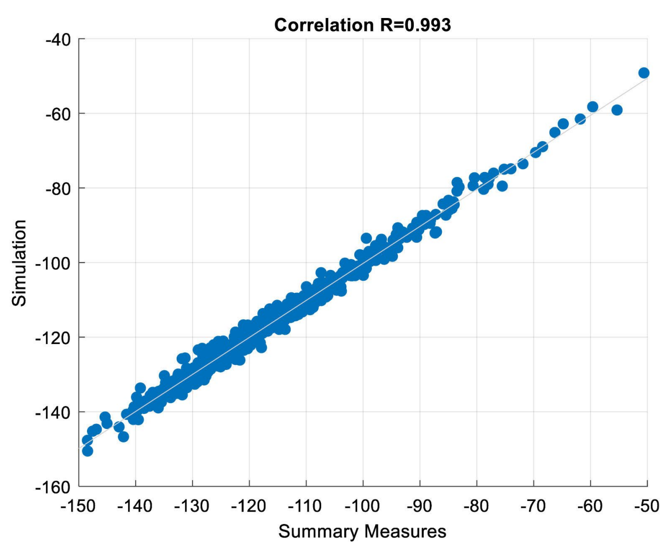

Figure 21. Pearson's correlation.

Figure 21 shows a regression line close to the diagonal, indicating a strong correlation. The Pearson correlation coefficient ≈ 1 and $p < 0.05$ indicate a statistically significant p-value, reflecting excellent agreement between the synthetic reference data and the predictions obtained through simulation. The closer the Pearson coefficient is to one, the more accurately the model reproduces the observed variations in received power levels.

➢ **Bland-Altman plot**

Figure 22 shows the Bland-Altman plot, which assesses the agreement between the synthetic reference data and the simulation. The limits—mean, $+1.96\sigma$, and -1.96σ enclose the observations.

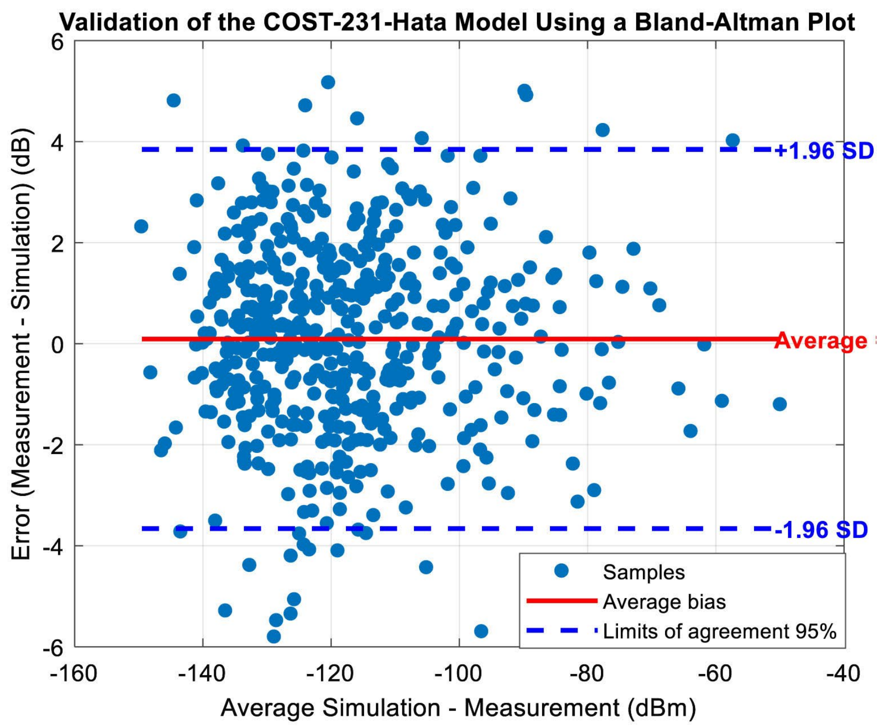

Figure 22. Bland-Altman plot for the COST-231 Hata Model.

Figure 22 shows a high concentration of samples around the mean bias (0.09 dB), combined with narrow agreement limits, indicating good stability and excellent precision of the model. These results support those obtained using the RMSE and Pearson's correlation coefficient, thereby confirming the statistical robustness and predictive reliability of the proposed COST-231 Hata model.

Correlation

Pearson R = 0.9933 (p = 0.00000)

MAE = 1.52 dB

NSE = 0.9867

The statistical results indicate good internal consistency of the COST-231 Hata model, enhanced by spatially correlated log-normal shadowing. The strong Pearson correlation ($R = 0.9933$; $p < 0.05$), low RMSE (1.52 dB), high NSE (0.988), and low Bland-Altman bias (0.09 dB) demonstrate satisfactory agreement between the simulations and the synthetic reference data. However, these metrics result from an internal evaluation based on simulated data and do not constitute independent experimental validation. The multicell coverage rate of 63.3% confirms the model's consistency within the studied framework, but field measurement campaigns are still necessary to verify its predictive accuracy and operational applicability to Guinean LTE networks operating around 1800 MHz.

3.3. Comparative Analysis of the Okumura-Hata and COST-231 Hata Models

Both the Okumura-Hata and COST-231 Hata models can be used to model radio coverage in LTE networks by incorporating the effects of spatially correlated log-normal shadowing as well as a multicellular architecture. However, their areas of validity and performance differ significantly, which affects their relevance for studies on the optimization of 4G LTE networks. Table 5 presents a comparative summary of the main results obtained and highlights the criteria justifying the choice of the COST-231 Hata model for simulations conducted at 1800 MHz. The most notable differences concern the frequency adaptation to 1800 MHz LTE networks and the multicellular coverage results obtained.

Table 5. Comparison of the results from the propagation models.

Comparison Criteria	Okumura-Hata	COST-231 Hata	Comparative Analysis
Frequency band	≤1500 MHz	1500 à 2000 MHz	COST-231 Hata is better suited for 1800 MHz LTE networks
Propagation loss	Good modeling	Very good modeling	Both models show a logarithmic increase consistent with propagation theory
RSRP	Gradual decrease with distance	Gradual decrease with distance	Both models accurately simulate the attenuation of the radio signal
SINR	Good representation of interference	Good representation of interference	COST-231 Hata is better suited for dense LTE networks
Probability of Coverage	Gradual decline	Gradual decline	Both models correctly distinguish between urban, suburban, and rural environments
Spatially Correlated Shadowing	Oui	Oui	Both models enhance the realism of radio simulations
Multi-cell coverage	45.5%	68.3%	COST-231 Hata offers better coverage, with a gain of 22.8 percentage points compared to Okumura-Hata.
Environmental Remedial Measures Tailored to Guinea	Oui	Oui	Both models take into account Guinea's specific geographic characteristics
Pearson's correlation	0.9933	0.9933	Very strong agreement between simulations and synthetic reference data

Continued

MAE	1.52 dB	1.52 dB	Low average absolute error for both models
NSE	0.9867	0.9882	Both models demonstrate excellent predictive power
Bland-Altman Plot	Bias = 0.09 dB	Bias = 0.09 dB	Very good statistical stability of the predictions
Statistical validation	Very satisfactory	Excellent	COST-231 Hata offers slightly better performance
Compatibility with 1800 MHz LTE Networks	Limited	Excellent	A significant advantage of the COST-231 Hata model
Recommended Model	A good reference model	Best Choice	COST-231 Hata is the most relevant for this study

Both the Okumura-Hata model and the COST-231 Hata model perform well in modeling LTE radio propagation phenomena. The statistical metrics obtained (Pearson > 0.99, MAE = 1.52 dB, and NSE > 0.98) demonstrate their robustness and predictive capability. However, the COST-231 Hata model stands out for its significantly higher multi-cell coverage (68.3% versus 45.5%) as well as its better adaptation to LTE frequencies around 1800 MHz. The inclusion of spatially correlated log-normal shadowing and environmental corrections specific to the Guinean context further reinforces the relevance of this model for radio planning and optimization studies. Based on the results obtained, the COST-231 Hata model is the most appropriate choice for the analysis and optimization of 4G LTE networks in the geographical context of Guinea.

4. Conclusions

This study compared the Okumura-Hata and COST-231 Hata models for simulating LTE propagation in urban, suburban, and rural environments. The incorporation of spatially correlated log-normal shadowing allows for a more realistic representation of spatial variations in the radio channel within the chosen simulation framework. The statistical metrics calculated from synthetic reference data show good internal consistency between the simulated results and the numerical references used. However, these results do not constitute independent experimental validation.

At 1800 MHz, the COST-231 Hata model appears theoretically more appropriate than the Okumura-Hata model due to its operating frequency range. Nevertheless, confirming this suitability in Guinean environments requires a campaign of real-world LTE measurements, including, in particular, RSRP, SINR, distance to the base station, antenna height, load conditions, and local topographical and vegetation characteristics.

The results presented should therefore be considered as a comparative modeling study and as a methodological basis for future experimental validation campaigns in Guinea.

Authors' Contributions

Kadiatou Aissatou Barry, Design and formulation of the research problem; literature review; development of the methodology; mathematical modeling of the Okumura-Hata and COST-231 Hata models; implementation of simulations in MATLAB; analysis and interpretation of the results; initial drafting and revision of the manuscript; Mohamed Ansoumane Camara, Contribution to the methodology for modeling radio propagation; support for the comparative analysis of models; critical review and improvement of the manuscript's scientific quality; coordination of the submission and publication process. Boudal Niang, Gucontributedhe research problem; supervision of the development of propagation models; contribution to the analysis and interpretation of results; critical review and scientific validation of the manuscript; Mamadou Sadigou Diallo, Contributed to the literature review; assisted with the analysis of LTE propagation models; contributed to the interpretation of the results; reviewed and revised the manuscript; Ismaila Diakhaté, Contributed to the literature review and methodological analysis; provided support for the study of radio propagation parameters; participated in the scientific review and refinement of the manuscript; Souleymane Soumah, contributed to the literature review; assisted with the analysis of simulation results; participated in the critical review and refinement of the manuscript's scientific presentation.

Conflicts of Interest

The authors declare no conflicts of interest regarding the publication of this paper.

References

[1] Hassan, R.S., Rahman, T.A. and Abdulrahman, A.Y. (2014) LTE Coverage Network Planning and Comparison with Different Propagation Models. *TELKOMNIKA* (*Telecommunication Computing Electronics and Control*), **12**, 153-162. https://doi.org/10.12928/telkomnika.v12i1.1794

[2] Global System Mobile Association GSMA (2024) The Mobile Economy Sub-Saharan Africa 2024. https://event-assets.gsma.com/pdf/GSMA_ME_SSA_2024_Web.pdf

[3] Barry, K., Soumah, S., Diallo, M., Camara, M., Diallo, A. and Barry, M. (2025) Multi-Parametric Analysis of the Coverage and Quality of Service (QoS) of 3G/4G Networks in the Sub-Saharan Environment: The Case of the Republic of Guinea. *Science Journal of Energy Engineering*, **13**, 154-166. https://doi.org/10.11648/j.sjee.20251303.16

[4] Gomez, S., Pajusco, P. and Person, C. (2015) Utilisation de modèles de propagation pour la prévision de l'exposition de personnes aux champs électromagnétiques. https://hal.science/hal-01185701v1/document

[5] Michel, D.D.E. and Emmanuel, T. (2015) Optimisation du modèle d'Okumura Hata par la régression linéaire. Application à la ville de Yaoundé au Cameroun. *IOSR Journal of Electronics and Communication Engineering* (*IOSR-JECE*), **10**, 63-72. https://urls.fr/YTyKag

[6] Noh, S.K. and Choi, D. (2019) Propagation Model in Indoor and Outdoor for the LTE Communications. *International Journal of Antennas and Propagation*, **2019**, Article ID: 134613. https://doi.org/10.1155/2019/3134613

[7] Gadze, J.D., Agyekum, K.A., Nuagah, S.J. and E.A. Affum, (2019) Improved Propagation Models for LTE Path Loss Prediction in Urban & Suburban Ghana. *International Journal of Wireless & Mobile Networks*, **11**, 35-53. https://doi.org/10.5121/ijwmn.2019.11603

[8] Nkordeh, Atayero, Idachaba et Oni (2014) LTE Network Planning Using the Hata-Okumura and the COST-231 Hata Pathloss Models. https://www.iaeng.org/publication/WCE2014/WCE2014_pp705-709.pdf

[9] Hicham, H.M. (2017) Etudes et modélisation des performances des réseaux LTE/LTE-A: vers le Handover. https://dspace.univ-tlemcen.dz/server/api/core/bitstreams/0c1b66c0-800c-4ad9-98e4-6645eb9b7b15/content

[10] Kindbelle Tossou, K.E.F. (2025) Optimisation de la qualité de service du réseau 4G au TOGO. https://theses.hal.science/tel-05526858v1/file/UTBM_These_TOSSOU_Kodjo_2025BELF0004.pdf

[11] Nuagah, S.J. Spearman 1904—The Proof and Measurement of Association between Two Things. https://webspace.ship.edu/pgmarr/Geo441/Readings/Spearman%201904%20-%20The%20Proof%20and%20Measurement%20of%20Association%20between%20Two%20Things.pdf

[12] Akanni, O., Samuel, O., Adewale, O., Adebayo, A.W. and Adekunle, J. Optimization of COST-231 Hata Radio Propagation Prediction Model for GSM 4G FDD-LTE Operating at 1800 MHz in Tropical Region. https://www.questjournals.org/jrme/papers/vol8-issue12/08120108.pdf

[13] Traore, M.M., Wane, D., Camara, I., Millimono, T.N., Kanté, I.K., Barry, M.B., *et al.* (2025) Characterization of Precipitation Indices in the Republic of Guinea Using *in-Situ* Data. *Atmospheric and Climate Sciences*, **15**, 941-955. https://doi.org/10.4236/acs.2025.154047

[14] Adekunle, A., Abimiku, Y.K., Umeobika, N.M. and Ameh, E.E. (2018) Radio Wave Detection Using Cost 231-Hata Model for Wireless Network Planning; a Case Study of Senate Building Environs of Unilag, Nigeria. *International Journal of Advances in Scientific Research and Engineering*, **4**, 107-113. https://doi.org/10.31695/ijasre.2018.32992

[15] (2009) Recommandation UIT-R P.1546-4—Méthode de prévision de la propagation point à zone pour les services de Terre entre 30 MHz et 3 000 MHz. https://www.itu.int/dms_pubrec/itu-r/rec/p/R-REC-P.1546-4-200910-S!!PDF-F.pdf

[16] Khatun, E. Comparative Analysis of Okumura-Hata and Cost 231 Path Loss Models for Wireless Mobile Communications. http://103.133.167.5:8080/bitstream/handle/123456789/2484/Eliza%20_Khatun.pdf?sequence=1&isAllowed=y

[17] Kumari, M., Yadav, T. and Yadav, P. (2011) Comparative Study of Path Loss Models in Different Environments. *International Journal of Engineering Science and Technology*, **3**, 2945-2949. https://urls.fr/HXVjM-

[18] Abdullahiand, M.B., Haulat, S.A., Abdullahi, M.B. and Haulat, S.A. (2025) Comparative Analysis and Optimization of Okumura-Hata and COST 231 Propagation Models with Field Measurements in Sokoto Metropolis, Nigeria. *International Journal of Advances in Engineering and Management*, **7**, 145-149. https://doi.org/10.35629/5252-0705145149

[19] Godo, M.H., Adja, G.M. and Assohoun, S.E. (2022) Optimisation des modèles de

propagation des ondes radioélectriques des réseaux mobiles de télécommunication en contexte de dynamique spatiotemporelle du tissu urbain: Cas de la Commune de Marcory dans le District d'Abidjan en Côte d'Ivoire. *Afrique SCIENCE*, **21**, 1-20. https://www.afriquescience.net/admin/postpdfs/d65c65f8a3fe99396f86814c96d0173d1719974537.pdf

[20] Das, A.X. and Sharma, S. (2018) Effective Analysis of various Radio Propagation Models in Wireless Sensor Network Scenario using Qualnet 6.1 Simulator. *Journal of Emerging Technologies and Innovative Research*, **5**, 261-272. https://www.jetir.org/papers/JETIR1812B36.pdf

[21] Salah, Y. (2021) Optimisation des positions des drones dans un réseau 5G en utilisant le GWO. https://bucket.theses-algerie.com/files/repositories-dz/2226536412589823.pdf

[22] Singh, Y. (2012) Comparison of Okumura, Hata and COST-231 Models on the Basis of Path Loss and Signal Strength. *International Journal of Computer Applications*, **59**, 37-41. https://doi.org/10.5120/9594-4216

[23] Autorité de Régulation des Postes et Télécommunications (ARPT) (2023) Mission d'Audit de la QoS des Opérateurs de Téléphonie Mobile et Fournisseurs d'Accès Internet . https://www.arpt.gov.gn/mission-daudit-de-la-qos-des-operateurs-de-telephonie-mobile-et-fournisseurs-dacces-internet-en-republique-de-guinee/

[24] Dinesh, D., *et al*. (2026) The Defence S&T Technical Bulletin, 19. https://www.google.com/url?sa=t&source=web&rct=j&opi=89978449&url=https://s741355ba672f4119.jimcontent.com/download/version/1773363485/module/15004615227/name/Ludovici_2026_vol_19_num_1.pdf&ved=2ahUKEwjpyPrJ7_-WAxWbWEEAHc4PI-JoQFnoECBgQAQ&usg=AOvVaw2j-tvOmItjI0UmAyn4HYL0

[25] Eisenblatter, A., Fugenschuh, A., Geerdes, H.F., Koch, T. and Martin, A. Optimization Methods for UMTS Radio Network Planning. https://opus4.kobv.de/opus4-matheon/frontdoor/deliver/index/docId/4/file/5.pdf

[26] Rappaport, T.S. (2009) Wireless Communications: Principles and Practice, 2ne Edition. Prentice Hall. https://telkom2013.wordpress.com/wp-content/uploads/2014/02/wireless-comm-princip-n-practice-theodoresrappaport.pdf

[27] Dieu, U.J.D. and Vianney, N.J.M. (2016) Characterization and Modeling of Large-Scale Fading for Radio Propagation in Rwanda. *Communications and Network*, **08**, 22-30. https://doi.org/10.4236/cn.2016.81003

[28] Kommission, E. (1999) Digital Mobile Radio towards Future Generation Systems: Cost Action 231; Final Report in Cost Telecommunications. Office for Official Publications of the European Communities. https://interactca20120.org/wp-content/uploads/2023/11/COST-Action-231-_-Digital-mobile-radio-towards-future-generation-systems-Final-report.pdf

[29] TELECOM ParisTech: BdL-TDMA-CDMA-OFDMA-4p.ppt. https://marceaucoupechoux.wp.imt.fr/files/2018/02/BdL-TDMA-CDMA-OFDMA-4p.ppt.pdf

[30] HiCellTek (2026) RSRP, RSRQ, SINR: Valeurs normales et interprétation pour 4G et 5G. HiCellTek. https://hicelltek.com/blog/rsrp-rsrq-sinr-valeurs-normales/

[31] Chai, T. and Draxler, R.R. (2014) Root Mean Square Error (RMSE) or Mean Absolute Error (MAE)? Arguments against Avoiding RMSE in the Literature. *Geoscientific Model Development*, **7**, 1247-1250. https://doi.org/10.5194/gmd-7-1247-2014

[32] Thunis, P., Pederzoli, A. and Pernigotti, D. (2012) Performance Criteria to Evaluate Air Quality Modeling Applications. *Atmospheric Environment*, **59**, 476-482. https://doi.org/10.1016/j.atmosenv.2012.05.043

[33] Hodson, T.O. (2022) Root-Mean-Square Error (RMSE) or Mean Absolute Error (MAE): When to Use Them or Not. *Geoscientific Model Development*, **15**, 5481-5487. https://doi.org/10.5194/gmd-15-5481-2022

[34] Kabela, E.D. and Carbone, G.J. (2015) NARCCAP Model Skill and Bias for the Southeast United States. *American Journal of Climate Change*, **4**, 94-114. https://doi.org/10.4236/ajcc.2015.41009

[35] Spearman, C. (2026) The Proof and Measurement of Association between Two Things. *The American Journal of Psychology*, **15**, 72-101. http://digamoo.free.fr/spearman1904a.pdf

[36] Gupta, H.V., Sorooshian, S. and Yapo, P.O. (1999) Status of Automatic Calibration for Hydrologic Models: Comparison with Multilevel Expert Calibration. *Journal of Hydrologic Engineering*, **4**, 135-143. https://doi.org/10.1061/(asce)1084-0699(1999)4:2(135)

[37] Efron, B. and Tibshirani, R. (1998) An Introduction to the Bootstrap. Chapman & Hall. https://www.hms.harvard.edu/bss/neuro/bornlab/nb204/statistics/bootstrap.pdf

[38] Efron, B. (1979) Bootstrap Methods: Another Look at the Jackknife. *The Annals of Statistics*, **7**, 1-26. https://doi.org/10.1214/aos/1176344552

Abbreviations

2D	2-Dimensional
4G-LTE	4th generation-Long Term Evolution
5G	5th generation
6G	6th generation
BS	Base Station
BTS	Base Transceiver Station
COST	European Cooperation in Science and Technology
ECC-33	Electronic Communications Committee-Model 33
eNodeB	Evolved Node
FSS-LMS	Fixed Satellite Service-Land Mobile Service
FSPL	Free Space Path Loss
ISD	Inter-Site Distance
LTE-A	Long Term Evolution-Advanced
MAE	Mean Absolute Error
NSE	Nash-Sutcliffe Efficiency
QoS	Quality of Service
RMSE	Root Mean Square Error
RSRP	Reference Signal Received Power
Rx	Receive
SIG	Système d'Information Géographique
SINR	Signal to Interference plus Noise Ratio
SUI	Stanford University Interim
Tx	Transmit
UE	User Equipment-terminal mobile
VS-LMS	Vehicular Service-Land Mobile Service